

Virial Masses of Black Holes from Single Epoch Spectra of AGN

Brandon C. Kelly and Jill Bechtold

bkelly@as.arizona.edu, jbechtold@as.arizona.edu

Steward Observatory, University of Arizona, 933 N Cherry Ave, Tucson, AZ 85721

ABSTRACT

We describe the general problem of estimating black hole masses of AGN by calculating the conditional probability distribution of M_{BH} given some set of observables. Special attention is given to the case where one uses the AGN continuum luminosity and emission line widths to estimate M_{BH} , and we outline how to set up the conditional probability distribution of M_{BH} given the observed luminosity, line width, and redshift. We show how to combine the broad line estimates of M_{BH} with information from an intrinsic correlation between M_{BH} and L , and from the intrinsic distribution of M_{BH} , in a manner that improves the estimates of M_{BH} . Simulation was used to assess how the distribution of M_{BH} inferred from the broad line mass estimates differs from the intrinsic distribution, and we find that this can lead to an inferred distribution that is too broad. We use these results and a sample of 25 sources that have recent reverberation mapping estimates of AGN black hole masses to investigate the effectiveness of using the C IV emission line to estimate M_{BH} and to indirectly probe the C IV region size–luminosity (R – L) relationship. A linear regression of $\log L_{\lambda}(1549\text{\AA})$ on $\log M_{BH}$ found that $L_{1549} \propto M_{BH}^{1.17 \pm 0.22}$. A linear regression also found that $M_{BH} \propto L_{1549}^{0.41 \pm 0.07} FWHM_{CIV}^2$, implying a C IV R – L relationship of the form $R_{CIV} \propto L_{1549}^{0.41 \pm 0.07}$. Including the C IV line $FWHM$ resulted in a reduction of a factor of $\sim 1/3$ in the error in the estimates of M_{BH} over simply using the continuum luminosity, statistically justifying its use. We estimated M_{BH} from both C IV and $H\beta$ for a sample of 100 sources, including new spectra of 29 quasars. We find that the two emission lines give consistent estimates if one assumes $R \propto L_{UV}^{1/2}$ for both lines.

Subject headings: galaxies: active — line: profiles — methods: data analysis — methods: statistical — quasars: emission lines

1. INTRODUCTION

It is widely accepted that the extraordinary activity associated with quasars involves accretion onto a supermassive black hole (SMBH). Furthermore, the evidence that almost all massive galaxies host SMBHs has become quite convincing. It has been found that SMBH mass is correlated with the host galaxy’s bulge luminosity (e.g., Kormendy & Richstone 1995; Magorrian et al. 1998; McLure & Dunlop 2001; Marconi & Hunt 2003) as well as the stellar velocity dispersion (e.g., Gebhardt et al. 2000a; Merritt & Ferrarese 2001; McLure & Dunlop 2002; Tremaine et al. 2002). Because luminous quasars have been observed to reside in massive early-type galaxies (McLure et al. 1999; Kukulka et al. 2001; McLeod & McLeod 2001; Nolan et al. 2001; Percival et al. 2001; Dunlop et al. 2003), this implies that the evolution of spheroidal galaxies and quasars is intricately tied together (e.g., Silk & Rees 1998; Haehnelt & Kauffmann 2000; Adams et al. 2001; Merritt & Poon 2004; Di Matteo et al. 2005). Therefore, understanding the cosmic evolution of SMBHs is an important task of modern astronomy.

Reverberation mapping (Blandford & McKee 1982; Peterson 1993) is often used to estimate SMBH mass, M_{BH} , in Type 1 active galaxies (Wandel et al. 1999; Kaspi et al. 2000; Peterson et al. 2004). One of the principal advantages of this method is that it does not require high spatial resolution, but rather relies on the time lag between the continuum and emission line variability. Under the assumption that the broad line region (BLR) is in Keplerian motion, the time lag is combined with the line width to give an estimate of SMBH mass. This, in principal, makes it immediately applicable for both faint and distant quasars. Although there are many potential systematic uncertainties in the technique (Krolik 2001), there has been good agreement between SMBH masses inferred from reverberation mapping and those inferred from the stellar velocity dispersion (Gebhardt et al. 2000b; Ferrarese et al. 2001; Nelson et al. 2004; Onken et al. 2004).

Unfortunately, reverberation mapping requires long-term intensive monitoring, which is not practical for large samples. In addition, the long time scales for variability in bright high redshift sources make reverberation mapping for these sources unfeasible. Fortunately, a correlation has been found that relates the BLR size and monochromatic continuum luminosity (the R - L relationship, Kaspi et al. 2000, 2005), making it possible to estimate virial masses from single-epoch spectra using the $H\beta$ width (Wandel et al. 1999). In addition, Wu et al. (2004) find a relationship between BLR size and the luminosity of $H\beta$, but Woo & Urry (2002) do not find any correlation between SMBH mass and bolometric luminosity. $H\beta$ is redshifted into the near-infrared at $z \sim 0.9$, making it difficult to observe from the ground for large samples. Vestergaard (2002) and McLure & Jarvis (2002) have argued for the use of C IV and Mg II, respectively, to estimate virial masses from single-epoch spectra, allowing quasar SMBH masses to be estimated at high z from the ground. Many studies have exploited these results and estimated SMBH masses for large samples of quasars (e.g., Bechtold et al. 2003; Corbett et al. 2003; Warner et al. 2003; Vestergaard 2004; McLure & Dunlop 2004; McLure & Jarvis 2004). Dietrich & Hamann (2004) have found that the estimates based on $H\beta$ and C IV agree well for high z quasars, whereas Mg II-based estimates are typically a factor of ~ 5 times lower. In contrast to this, Shemmer et al. (2004) and Baskin & Laor (2005) argue that C IV does not give as accurate of an estimate of SMBH mass as $H\beta$.

Previous methods that utilize single-epoch spectra have relied on empirical linear relationships that estimate the BLR size for a given source luminosity, and then use this estimate of R in the virial relationship. Although this will give good estimates for R , this may give less efficient estimates for SMBH mass. The reason for this is that the luminosity may also be correlated with M_{BH} in a manner independent of the R - L relationship, such as through the accretion process. By only using the luminosity as a proxy for R when estimating M_{BH} , one is ignoring the additional information of M_{BH} that is contained within L . In other words, the standard broad line estimates are based on the distribution of velocities at a given luminosity and M_{BH} , as folded through the R - L correlation and under the assumption of Keplerian motion. However, the distribution of black hole masses at a given luminosity and line width is not simply obtained by inverting the distribution of velocities at a given luminosity and black hole mass, unless L and M_{BH} are statistically independent.

Recent studies have found evidence for a correlation between luminosity and black hole mass (e.g., Corbett et al. 2003; Netzer 2003; Peterson et al. 2004), suggesting that black hole mass and luminosity are not statistically independent. However, in contrast to other studies, Woo & Urry (2002) have argued that there is no significant correlation between bolometric luminosity and M_{BH} . If a correlation between M_{BH} and L exists, then we can combine the M_{BH} - L correlation with the broad line mass estimates to obtain, on average, more accurate estimates of M_{BH} for a given luminosity and line width.

In this work, we outline a formalism that allows one to estimate the probability distribution of an AGN's

black hole mass, given some set of observables. We focus on the special case of estimating M_{BH} given some monochromatic luminosity, L_λ , and the width of an emission line. We also search for other parameters of the C IV line that may contribute additional information of M_{BH} , thus decreasing the uncertainty in the estimated M_{BH} . Although it is possible to include other quasar properties, such as radio loudness, X-ray loudness, or variability (e.g., Xie et al. 2005; O’Neill et al. 2005; Pessah 2006), for simplicity we have chosen to only include parameters that may be measured from a single spectrum containing C IV. This allows M_{BH} to be estimated using only one spectrum, and it is thus not necessary to compile observations from several different spectral regions.

We use the formalism developed here to justify using the C IV line width in estimating M_{BH} , and attempt to indirectly infer the C IV R – L relationship. We have chosen the C IV line because it is readily observable from the ground over a wide range in redshift ($1.5 \lesssim z \lesssim 4.5$), is less effected by blends with iron and other lines, has shown to give consistent mass estimates with H β (Vestergaard 2002), is commonly employed to estimate SMBH mass, and archival UV spectra are available for most of the sources with reverberation-based masses (Peterson et al. 2004). Despite its common usage, the R – L relationship for C IV is mostly unexplored, as there are only seven data points with reliable C IV reverberation mapping data (Peterson et al. 2005). Often it is assumed that C IV BLR size has the same dependence on luminosity as H β (e.g., Vestergaard 2002; Netzer 2003; Vestergaard & Peterson 2006). Another possibility is to assume $R \propto L^{1/2}$, as predicted from simple photoionization theory or if the BLR size is set by the dust sublimation radius (Netzer & Laor 1993); this was done by Wandel et al. (1999) and Shields et al. (2003) for the H β line. Peterson et al. (2005) performed a linear regression using five AGN with a total of seven data points and find $R \propto L_{UV}^{0.61 \pm 0.05}$, similar to that for the Balmer lines¹. Unfortunately, this result is almost entirely dependent on the inclusion of NGC 4395, the least luminous known Seyfert 1 galaxy, since the data points for the other AGN are clustered around $\lambda L_\lambda(1350\text{\AA}) \approx 10^{43.75}$ ergs s^{−1}. Vestergaard & Peterson (2006) found that using the C IV line to calculate black hole masses assuming $R \propto L_{UV}^{0.53}$ gave results consistent with masses obtained by reverberation mapping.

The layout of the paper is as follows. In § 2 we describe the general problem of estimating SMBH mass from single-epoch spectra, and in § 3 we describe our two samples. The first sample is a set of 25 quasars with black holes from reverberation mapping and archival UV spectra, and the second sample is a set of 100 quasars for which we have spectra containing both the H β and C IV emission lines. In § 4 we describe the method we employ to estimate the emission line parameters. In § 5 we test if any other UV or C IV parameters contribute useful information about M_{BH} . In § 6.1 we use the sample with reverberation mapping data to investigate the M_{BH} – L relationship, and in § 6.2 we test if including the C IV line $FWHM$ is preferred by this sample and investigate the nature of the C IV R – L relationship. In § 7 we use our larger sample to compare estimates of M_{BH} obtained from both single-epoch H β and C IV. We summarize our results in § 8.

In this work we adopt the WMAP best-fit cosmological parameters ($h = 0.71, \Omega_m = 0.27, \Omega_\Lambda = 0.73$, Spergel et al. 2003). We will use the common statistical notation where a point estimate of a quantity is denoted by placing a $\hat{\cdot}$ above it, e.g., \hat{M}_{BH} would be an estimate of M_{BH} . We will also commonly refer to the bias of an estimate, where the bias of \hat{M}_{BH} is $Bias = E(\hat{M}_{BH}) - M_{BH}$. Here, $E(\hat{M}_{BH})$ is the expectation value of \hat{M}_{BH} . An unbiased estimate of M_{BH} is one such that $E(\hat{M}_{BH}) = M_{BH}$.

¹This value appears in an erratum to this paper

2. ESTIMATING BLACK HOLE VIRIAL MASSES

If one assumes that the BLR gas is in Keplerian motion, then the mass of the central black hole, M_{BH} , may be estimated from the virial theorem :

$$M_{BH} = f \frac{RV^2}{G}. \quad (1)$$

Here R is the distance between the BLR that is emitting a particular line and the central continuum source, V is the velocity dispersion of the line-emitting gas, and G is the gravitational constant. The velocity dispersion is inferred from the width of the line, quantified using either the *FWHM* or line dispersion, σ_* . The factor f is a scaling factor that converts the virial product, RV^2/G , to a mass. Typically, f has been set to the value appropriate for an isotropic velocity field, where $f = 3/4$ if one uses the broad line *FWHM* to estimate V (e.g., Netzer 1990); however, there may be systematic effects that can significantly effect the value of f (Krolik 2001). Onken et al. (2004) used the correlation between M_{BH} and stellar velocity dispersion to estimate an average scale factor of $\langle f \rangle = 5.5$ when the line dispersion is used to estimate V . For simplicity, in the rest of this work we will assume $f = 1$, so that what is really being estimated is the virial product. After estimating the virial product, we can convert it to a mass using any adopted value of f .

2.1. Estimating M_{BH} from Reverberation Mapping

For the case of reverberation mapping, estimating M_{BH} is straightforward. The BLR size, R , can be estimated as $c\tau$, where c is the speed of light and τ is either the peak or the centroid of the line–continuum cross-correlation function. The velocity dispersion of the line-emitting gas, V , is estimated from the width of the broad emission line as measured in the variable part of the spectrum. Measuring V from the variable (RMS) spectrum ensures that one is probing the line emission that is actually varying, i.e., the BLR gas that is at the distance $c\tau$. One then uses $c\tau$ and V in Equation (1) to estimate M_{BH} . See Peterson et al. (2004) for recent reverberation mapping results.

2.2. Estimating M_{BH} from Single-Epoch Spectra

Estimating M_{BH} from a single-epoch spectrum (SES) is a somewhat different problem for several reasons. In this section we illustrate why the SES case is different, and provide a general formalism for calculating the conditional probability distribution of M_{BH} , given a set of observables.

In the single-epoch case, one cannot directly observed the BLR size, but instead employs a correlation between R and continuum luminosity. However, there is considerable scatter in the R – L relationship, which is propagated through when using L instead of R to estimate M_{BH} . In this case, the conditional probability distribution of M_{BH} , given the broad line estimate, is broad, typically a factor of a few (Vestergaard 2002; Kaspi et al. 2005). This scatter can be reduced by incorporating information about M_{BH} from other observables. In the more general case, one may have several parameters that contain information about M_{BH} , such as emission line width, variability, luminosity, etc. For example, Merloni et al. (2003) have found evidence that black hole mass is correlated with X-ray and radio luminosity. In this case, one could combine the information from the line width, UV luminosity, X-ray luminosity, and radio luminosity to obtain an estimate of M_{BH} that is more accurate than would have be obtained solely from some subset of these parameters.

To be more specific, suppose that one has a set of observables, denoted by X . Then, given the observables, X , the conditional probability of M_{BH} given X is given by Bayes' Formula

$$p(M_{BH}|X) = \frac{p(X|M_{BH})p(M_{BH})}{p(X)}, \quad (2)$$

where $p(M_{BH})$ is the intrinsic probability distribution of M_{BH} for a sample, and $p(X)$ is the distribution of the observables; $p(X)$ is just a normalizing constant and may be ignored.

In this work we are concerned with the distribution of M_{BH} given L , the emission line width, and redshift. For this case, Equation (2) becomes

$$p(m|l, v, z) \propto p(v|l, m, z)p(l|m, z)p(m|z). \quad (3)$$

Here, we are using the notation, $m \equiv \log M_{BH}$, $l \equiv \log \lambda L_\lambda$, and $v \equiv \log V$. The first term, $p(v|l, m, z)$, is the distribution of line widths at a given l , m , and z . The second term, $p(l|m, z)$, is the distribution of luminosities at a given m and z . The last term, $p(m|z)$, is the distribution of m at a given redshift. As we will show later in this section, $p(v|l, m, z)$ is obtained by plugging the R - L relationship into the Virial theorem (Eq.[1]). This is the standard method of estimating M_{BH} from the broad lines, but it implicitly assumes $p(m|l, v, z) \propto p(v|l, m, z)$, and therefore that $p(m|z)$ and $p(l|m, z)$ are uniform. Taking $p(m|z)$ and $p(l|m, z)$ to be uniform results in a broader distribution of M_{BH} , given L , V , and z , and thus a less efficient, albeit still unbiased, estimate of M_{BH} . However, by incorporating information on both the distribution of luminosities at a given black hole mass and redshift, and the distribution of M_{BH} at a given redshift, one can obtain a better estimate of M_{BH} .

To estimate a functional form for $p(l|m)$ and $p(v|l, m, z)$, suppose we observe some quasar with SMBH mass M_{BH} at a redshift z , where m is drawn from some probability density $p(m|z)$, $m|z \sim p(m|z)$. We assume that the accretion process for this source generates a luminosity, $L_\lambda \propto M_{BH}^{\alpha_m(z)}$, by

$$l|m, z = \alpha_0 + \alpha_m(z)m + \epsilon_l(z, m). \quad (4)$$

Here, α_0 is some constant of proportionality, and $\epsilon_l(z, m)$ is the random error term representing the scatter about this relationship. We will refer to Equation (4) as the M_{BH} - L relationship. The stochastic term, $\epsilon_l(z, m)$, encompasses variations at a given M_{BH} in the accretion rate (\dot{M}), radiative efficiency (ϵ), source inclination, bolometric correction (C_{bol}), etc.; since we do not observe these quantities we model them as being random. For now, we allow the logarithmic slope, α_m , to depend on z , and the random error to depend on z and M_{BH} .

The parameter α_m can be predicted from accretion physics. The radiated bolometric luminosity from an accretion flow can be written as

$$L = (1.26 \times 10^{31}) \epsilon \dot{m} \frac{M_{BH}}{M_\odot} \text{ W}, \quad (5)$$

where $\dot{m} = \dot{M}/\dot{M}_{edd}$ is the accretion rate normalized to Eddington. If one assumes $L_\lambda = C_{bol}L$, then from Equation (5) it follows that for this case $\alpha_m = 1$ and $\epsilon_l = \log \epsilon + \log \dot{m} + \log C_{bol}$. A more careful analysis of the thin disk case suggests $\lambda L_\lambda \propto (M_{BH}\dot{M})^{\alpha_m}$, $\alpha_m = 2/3$, after employing some simplifying approximations (e.g., Collin et al. 2002).

Given this luminosity, the BLR distance R is assumed to be set by the luminosity according to the R - L relationship, $R \propto L^{\theta_l}$:

$$r|l, z = \theta_0 + \theta_l l + \epsilon_r(z). \quad (6)$$

Similar to above, $r \equiv \log R$ and $\epsilon_r(z)$ is the stochastic component. In Equation (6) we assume that given L , R is independent of M_{BH} . In addition, we have not assumed any redshift dependence for θ_l because it is likely that the form of the R – L relationship is independent of z (Vestergaard 2004). However, in Equation (6) we have allowed for the possibility of a redshift dependence for ϵ_r as the the intrinsic scatter in the R – L relationship may depend on z .

Simple photoionization theory predicts that $R \propto L_{ion}^{1/2}$, where L_{ion} is the luminosity of the ionizing continuum (e.g., Wandel et al. 1999; Kaspi et al. 2000). From the definition of the ionization parameter, U , it follows that

$$2r = \log L_{ion} - \log(4\pi c) - \log U - \log n_e - \log \bar{E}, \quad (7)$$

where \bar{E} is the average energy of an ionizing photon and n_e is the BLR gas density. If we make the simplifying assumptions that r is set by Equation (7), $L_\lambda \propto L_{ion}$, and the means of the distributions of U , n_e , and \bar{E} are independent of L_λ , then comparison with Equation (6) shows that $\theta_l = 1/2$ and $\epsilon_r = -\log U - \log n_e - \log \bar{E}$. If this is not the case, but rather the means of the distributions of U , n_e , and \bar{E} have a power-law dependence on L_{ion} , then Equation (7) is still valid, but in general $\theta_l \neq 1/2$. Either way, in this model the scatter about the R – L relationship is partly the result of variations in U , n_e , and \bar{E} . Other sources of scatter may include variations in the conversion between L_λ and L_{ion} , source inclination, and the non-instantaneous response of the BLR to continuum variations.

If R is set by the dust sublimation radius, then we also expect $\theta_l = 1/2$ (Netzer & Laor 1993), but in this case $R \propto L^{1/2}$. A relationship of the form $R \propto L_\lambda^{1/2}$ is consistent with the results of Peterson et al. (2004) for the Balmer lines if one uses the UV continuum luminosity.

Finally, from Equation (1) the observed SES line width depends on R and M_{BH} as

$$v|r, m = v_0 - \frac{1}{2}r + \frac{1}{2}m + \epsilon_v, \quad (8)$$

where, $v_0 = \log(\sqrt{G}/f_{SES})$, and ϵ_v is the stochastic term. The term f_{SES} converts the SES line width measurement into a velocity dispersion, and ϵ_v describes random deviations of single-epoch v from that for the RMS spectrum. Vestergaard (2002) has found that the single-epoch H β $FWHM$ and the RMS H β $FWHM$ are consistent with a scatter of $\sim 20\%$, if one does not subtract the SES H β narrow component. When the $FWHM$ is used, $f_{SES} \approx 1/2$. Through the stochastic terms ϵ_l , ϵ_r , and ϵ_v , Equations (4), (6), and (8) define the conditional probability densities that describe how L and V depend on M_{BH} , and how R depends on L .

It is useful to examine the special case of Gaussian error terms, ϵ_l , ϵ_r , and ϵ_v , and Gaussian $p(m|z)$. In this case, the distribution of m at a given l and v is also normal. If we assume that ϵ_l , ϵ_r , and ϵ_v are uncorrelated, have zero mean, and variances σ_l^2 , σ_r^2 , and σ_v^2 , respectively, then the optimal estimate of m is the mean of $p(m|l, v, z)$, μ . If we make the further assumption that ϵ_l , ϵ_r , and ϵ_v are independent of m and z , and that α_m does not depend on z , then $p(m|l, v, z)$ takes a particularly simple form. The mean of $p(m|l, v, z)$ may be calculated from the properties of the normal distribution (e.g., Gelman et al. 2004) as

$$\mu = \frac{\hat{m}_{BL}/\sigma_{BL}^2 + \hat{m}_{ML}/\sigma_{ML}^2 + \bar{m}(z)/\sigma^2(z)}{1/\sigma_{BL}^2 + 1/\sigma_{ML}^2 + 1/\sigma^2(z)}. \quad (9)$$

Here, $\hat{m}_{BL} = m_0^{BL} + \theta_l l + 2v$ is the standard broad line mass estimate, found by plugging Equation (6) into Equation (8), $m_0^{BL} = \theta_0 - 2v_0$, $\sigma_{BL}^2 = \sigma_r^2 + 4\sigma_v^2$ is the variance in \hat{m}_{BL} , $\hat{m}_{ML} = (l - \alpha_0)/\alpha_m$ is the estimate of m based on the M_{BH} – L relationship, $\sigma_{ML}^2 = \sigma_l^2/\alpha_m^2$ is the variance in \hat{m}_{ML} , $\bar{m}(z)$ is the mean m at a given z , and $\sigma^2(z)$ is the variance in m at a given z .

The variance in μ as an estimate for m , σ_μ^2 , is

$$\sigma_\mu^2 = \left(\frac{1}{\sigma_{BL}^2} + \frac{1}{\sigma_{ML}^2} + \frac{1}{\sigma^2(z)} \right)^{-1}. \quad (10)$$

As is apparent from Equation (10), the variance in μ as an estimate for m is always less than that for the standard broad line estimate, \hat{m}_{BL} . In fact, in the limit $(\sigma_{ML}^2, \sigma^2(z)) \rightarrow \infty$, $p(m|l)$ and $p(m|z)$ supply no information on the black hole mass and μ converges to the broad line estimate. However, by combining the broad line mass estimate with the information on M_{BH} that is contained within the luminosity and redshift we can obtain a better estimate of m .

In reality, the distribution of \dot{m} is unlikely to be Gaussian, and since \dot{m} is a component of ϵ_l , this would violate the assumption that ϵ_l is Gaussian. Instead, the distribution of \dot{m} is likely bimodal (Ho 2002; Marchesini et al. 2004; Hopkins et al. 2006; Cao & Xu 2006) as a result of a transition from a radiatively inefficient flow to an efficient one at $\dot{m} \sim 0.01$ (e.g., Jester 2005). However, because of the flux limits of modern surveys, most observed broad line quasars will have $\dot{m} \gtrsim 0.01$ (McLure & Dunlop 2004; Vestergaard 2004). This results in a unimodal, relatively smooth and symmetric distribution of \dot{m} for observed quasars (Hopkins et al. 2006). It may also be that BLRs do not form in sources with $\dot{m} \lesssim 10^{-3}$ (Nicastro et al. 2003; Czerny et al. 2004), and therefore the distribution of \dot{m} for broad line AGN would have a lower limit at $\dot{m} \sim 0.001$. If true, then unimodality in the distribution of \dot{m} for broad line AGN is ensured.

The stochastic scatter about the M_{BH} - L relationship, ϵ_l , is the sum of random deviations in \dot{m} , bolometric correction, radiative efficiency, etc. We assume that the distributions of most, if not all, of the constituent components of ϵ_l are not too different from a Gaussian distribution, i.e., unimodal, smooth, and fairly symmetric. Then, by the central limit theorem, the distribution of the sum of these components, ϵ_l , will tend toward a normal density. Therefore, without any evidence to the contrary, the normal density should provide an accurate approximation to the true form of $p(l|m)$. A similar argument may be used to justify the assumption of normality for ϵ_r and ϵ_v .

To illustrate the improvement that Equation (9) offers over the broad line mass estimate, we simulate values of m , l , and v . The simulations were performed as follows. First, we simulated values of m from a smoothly-connected double power-law, with a mean of $\bar{m} \approx 7.87$ and a dispersion of $\sigma \approx 0.45$ dex. Values of l were then generated according to Equation (4), with $\alpha_0 = 37, \alpha_m = 1$. The gaussian scatter about this relationship had a dispersion of 0.7 dex. Then, we generated values of v as $v = 11 - l/4 + m/2 + \epsilon$, where ϵ was a gaussian random variable with dispersion 0.2 dex. This form for v assumes $R \propto L^{1/2}$, and corresponds to an intrinsic scatter in the broad line mass estimates of 0.4 dex. The parameters for simulating l and v were chosen to be similar to the results found in § 6. Finally, we calculated broad line mass estimates from the simulated luminosities and line widths, $\hat{m}_{BL} = -22 + l/2 + 2v$, and mass estimates μ according to Equation (9).

The results are shown in Figure 1. As can be seen from the distribution of residuals, the mass estimates that combine all available information on the black hole mass, μ , are more accurate on average than the broad line estimates, \hat{m}_{BL} . In addition, the distribution of μ provides a more accurate estimate of the true distribution of m than does \hat{m}_{BL} , with the distribution of m inferred from \hat{m}_{BL} being too broad. It is interesting to note that both of these results are in spite of the fact that the intrinsic distribution of m is not Gaussian, which was assumed when deriving Equation (9). This suggests that if the intrinsic distribution of m for a sample is not too different from a normal density, Equation (9) will still give more efficient estimates than the broad line estimates. This is reasonable, considering that Equation (9) ‘shrinks’ the black hole mass estimates towards the sample mean by an amount inversely proportional to the intrinsic variance in m .

of a sample.

2.3. Cautions for Using Quantities Calculated from the SES Mass Estimates

The intrinsic uncertainty in M_{BH} inferred from L_λ and the line width may be thought of as the ‘measurement’ error in M_{BH} . This intrinsic uncertainty can cause problems when using the black hole mass estimates, \hat{m} , to calculate additional quantities. In particular, quantities based on the square of the estimated \hat{m} , such as correlation coefficients and linear regressions, can be significantly effected (e.g., see Akritas & Bershadsky 1996; Fox 1997).

Suppose we are interested in calculating the correlation between M_{BH} and some other parameter X . To estimate this correlation, we would obtain a sample of quasars with black hole masses estimated from some assumed form of $p(m|l, v, z)$, \hat{m} . Typically, these are the standard broad line estimates. We then calculate the correlation coefficient between X and \hat{m} . However, because we do not have the actual black hole masses for our sample, but instead obtained estimates from the continuum luminosities and widths of the broad lines, this is not the *true* correlation coefficient between X and m . Because our estimated black hole masses have been ‘measured’ with error, this broadens the observed distribution of black hole masses, and thus biases the observed correlation coefficient towards zero. Therefore, the correlation coefficient obtained from the estimated black hole masses will be, on average, *less* in magnitude than the correlation coefficient that would have been obtained using the actual black hole masses.

To prove this point, we note that the logarithmic black hole mass estimates are related to the actual black hole masses as $\hat{m} = m + \epsilon_m$, where ϵ_m is the random error between \hat{m} and m . The linear correlation between the parameter of interest X and m is $\rho = Covar(X, m)/[Var(X)Var(m)]^{1/2}$, where *Covar* and *Var* are the sample covariance and variance, respectively. Since we don’t actually observe m , we can’t calculate the true correlation coefficient, but instead we calculate the correlation between X and \hat{m} , $\hat{\rho}$. While the covariance between X and m is unaffected by using \hat{m} instead of m , the sample variance of \hat{m} is $Var(\hat{m}) = Var(m) + \sigma_{\hat{m}}^2$, where $\sigma_{\hat{m}}^2$ is the intrinsic uncertainty in \hat{m} as an estimate for m , $\sigma_{\hat{m}}^2 = E(\epsilon_m^2)$. The observed correlation is then given by

$$\hat{\rho} = \left[\frac{Var(m)}{Var(m) + \sigma_{\hat{m}}^2} \right]^{1/2} \rho \quad (11)$$

Therefore, correlation coefficients calculated using the estimated black hole masses will be reduced in magnitude from the true correlation by a factor of $[1 + \sigma_{\hat{m}}^2/Var(m)]^{-1/2}$. For broad line mass estimates based on H β , Vestergaard & Peterson (2006) find $\sigma_{\hat{m}} = 0.43$ dex. In this work we find that $\sigma_{\hat{m}} \approx 0.40$ dex for C IV-based broad line estimates. For a sample with an intrinsic dispersion in m of 0.75 dex, these values of $\sigma_{\hat{m}}$ correspond to a decrease in the magnitude of any observed correlation by $\approx 12\%$. If the sample has an intrinsic dispersion of 0.4 dex, similar to the intrinsic uncertainties in the broad line estimates, then the magnitude of the observed correlation coefficient is reduced by $\approx 30\%$. These effects is not negligible, and can be more serious for linear regression (e.g., Fox 1997). In light of these issues, care must be taken when calculating quantities from black hole mass estimates based on single-epoch spectra.

Another problem arises when one is using a flux limited sample to estimate the intrinsic distribution of the black hole mass, i.e., the active black hole mass function (Wang et al. 2006), based on broad line estimates. There is currently significant interest in this problem, as the active black hole mass function is an important tool in understanding SMBH formation and evolution. Unfortunately, the limiting flux of a survey causes incompleteness in black hole mass, the degree of which depends on the distribution of l at a

given m and z , $p(l|m, z)$. In addition, because the broad line mass estimates are measured with error, the distribution of m inferred from the broad lines can be significantly broader than the intrinsic distribution (cf., Fig.1). Because of these issues, estimates of the active black hole mass function obtained from broad line estimates should be interpreted with caution.

In order to estimate the degree of incompleteness in m , it is necessary to re-express the survey selection function as a function of m . Following Gelman et al. (2004), we introduce an indicator variable, I , denoting whether a source is included in the survey, where $I = 1$ if a source is included and $I = 0$ if a source is missed. Then the selection function of the survey is the probability that a source is included in the survey for a given luminosity and redshift, $p(I = 1|l, z)$. The selection function for black hole mass is then

$$p(I = 1|m, z) = \int_{-\infty}^{\infty} p(I = 1|l, z)p(l|m, z)dl. \quad (12)$$

As can be seen, estimating the completeness in m for a survey depends on the form of $p(l|m, z)$. Therefore, it is important to understand $p(l|m, z)$, even if such an understanding does not result in significantly better estimates of m .

3. THE SAMPLE

We employ two samples in our analysis. The first sample consists of a set of 25 low- z sources that have reverberation mapping data from Peterson et al. (2004). We use this sample to investigate the M_{BH} - L relationship and the C IV R - L relationship, and to justify using the C IV line to estimate AGN black hole masses. The second sample is a set of 100 quasars for which we have separate spectra containing the H β and C IV emission lines. We use this sample to compare the broad line estimates of M_{BH} obtained from the two lines.

Peterson et al. (2004) calculated virial products for 35 AGNs based on the reverberation mapping method. Of those 35 sources, we selected ones with archival UV spectra. We did not include those sources which Peterson et al. (2004) listed as having unreliable virial products (PG 0844+349, PG 1211+143, PG 1229+204, and NGC 4593). We also did not include NGC 3227 or NGC 4151, as the C IV line for these sources had significant absorption. In addition, we removed NGC 4051 from the analysis because this source is an outlier in the BLR R-L relationship (Vestergaard 2002; Kaspi et al. 2005), and thus probably does not follow the linear relationship assumed in Equation (6). Our sample consists of 25 AGN: 14 sources with HST FOS spectra, 9 sources with IUE spectra, 1 source with HST GHRS spectra, and 1 source with HST STIS spectra. Of the 14 sources with FOS spectra, 13 were taken from Bechtold et al. (2002), and the other (NGC 5548) from Evans & Koratkar (2004). For archival sources with more than one observation, we took the source with the longest exposure time. All spectra are single-epoch, except for NGC 5548, which is averaged over approximately a month of HST observations. The sample is summarized in Table 1.

The luminosities were calculated from the predicted continuum flux at 1549Å, assuming a power law continuum (see § 4.1). We corrected luminosities for galactic absorption using the $E(B - V)$ values taken from Schlegel et al. (1998), as listed in the NASA/IPAC Extragalactic Database (NED), and the extinction curve of Cardelli et al. (1989), assuming a value of $A_V/E(B - V) = 3.1$. We did not do this for the Bechtold et al. (2002) sources as they have already been corrected for galactic absorption. The C IV line widths for the IUE sources were corrected by subtracting an assumed instrumental resolution of 1000 km s⁻¹ in quadrature from the measured line widths; the resolution for the other instruments is negligible compared to the emission line widths, so no correction was performed.

We compiled UV and optical spectra for a sample of 100 sources for the purpose of comparing the C IV-based estimates derived here with the estimates based on H β and the empirical R – L relationship. Of these sources, 89 have $z < 0.8$, 6 have $z \sim 2.3$, and 2 have $z \sim 3.3$. The UV spectra for the $z < 0.8$ sources are FOS spectra from Bechtold et al. (2002), the optical spectra for 51 of these sources are from Marziani et al. (2003), and the optical spectra for 9 of these sources are from the SDSS DR2 (Abazajian et al. 2004). Optical spectra for the 29 remaining $z < 0.8$ sources were obtained by us. Twenty-seven of the sources were observed at the Steward Observatory 2.3m Bok Telescope on Kitt Peak using the 600 lines mm $^{-1}$ grating of the B&C Spectrograph; these sources had moderate spectral resolution ($\sim 5 \text{ \AA}$). The other two sources were observed at the Magellan Baade Telescope using the Inamori Magellan Areal Camera and Spectrograph (IMACS); long-slit spectra were obtained for these sources using a slit width of 0.9" in long camera mode. We used the 600 lines mm $^{-1}$ grating for PKS 1451-375 and the 300 lines mm $^{-1}$ grating for PKS 2352-342, giving spectral resolutions of $\sim 2 \text{ \AA}$ and $\sim 5 \text{ \AA}$, respectively. The log of new spectra is displayed in Table 2, and they are shown in Figure 4. The spectra were reduced using the standard IRAF routines.

Rest-frame UV spectra for the eight sources with $z > 2$ are from Scott et al. (2000) and the SDSS. The continuum luminosities and H β $FWHM$ for the $z \sim 2.3$ sources were taken from McIntosh et al. (1999) and corrected to our adopted cosmology. The continuum fluxes for the two $z \sim 3.3$ sources were measured directly off the published spectra of Dietrich et al. (2002), and the values of H β $FWHM$ for them are from Dietrich & Hamann (2004).

4. LINE PROFILE PARAMETERS

4.1. Extracting The Line Profile

In order to extract the C IV emission line, it is necessary to subtract the continuum, Fe emission, and the He II $\lambda 1640$ and O III] $\lambda 1665$ emission lines. To remove the continuum and iron emission, we use a variation of the method outlined in Boroson & Green (1992). We model the continuum as a power law of the form $f_\nu \propto \nu^\alpha$. The Fe emission was modeled as a scaled and broadened form of the Fe emission template extracted from I Zw I by Vestergaard & Wilkes (2001). In contrast to most previous studies, we simultaneously fit the continuum and Fe emission parameters using the Levenberg-Marquardt method for nonlinear χ^2 -minimization; this is similar to the method used by McIntosh et al. (1999). Performing the fits in this manner has the advantage of providing an estimate of the uncertainties in these parameters, given by the inverse of the curvature matrix of the χ^2 space. The set of possible windows used to fit the continuum and Fe emission are shown in Table 3. The actual continuum windows used to fit the continuum and Fe emission for any particular source depended on that source's available spectral range.

Having obtained an estimate of the continuum and Fe emission, we subtracted these components from each spectrum. We then extracted the region within $-2 \times 10^4 \text{ km s}^{-1}$ and $3 \times 10^4 \text{ km s}^{-1}$ of 1549 \AA . Here, and throughout this work, we will use the convention that negative velocities are blueward of a given wavelength. Narrow absorption lines were removed and interpolated over. We then removed the He II $\lambda 1640$ and O III] $\lambda 1665$ emission lines from the wings of the C IV profile. This was done by modelling the C IV, He II, and O III] lines as a sum of Gaussians. In general, C IV was modelled as a sum of three Gaussians, He II two Gaussians, and O III] a single Gaussian, however this varied from source to source. The C IV extraction was done interactively in order to ensure accuracy of the fits. After obtaining estimates of the He II and O III] profiles, we subtracted these components. We did not fit the N IV] $\lambda 1486$ emission line as this line is typically weak and lost in the C IV wings.

Extraction of the H β profile was done in a similar manner. For the optical Fe emission we used the I Zw I template of Véron-Cetty et al. (2004). After subtracting the continuum and Fe emission, we extracted the region within $\pm 2 \times 10^4$ km s $^{-1}$ of 4861Å. The H β profile was modeled as a sum of 2–3 Gaussians. The [O III] $\lambda 4959\text{Å}$ and [O III] $\lambda 5007\text{Å}$ lines were modeled as a sum of 1–2 Gaussians, depending on the signal-to-noise of the lines. A sum of two Gaussians was used for the higher S/N lines because the [O III] lines are not exactly Gaussian, and not because the separate Gaussians are considered to be physically distinct components. The widths of the narrow Gaussians for [O III] were fixed to be equal. The [O III] lines and the narrow H β line were then subtracted to extract the H β line. As with the C IV profile, the entire extraction was done interactively.

4.2. Estimating The Line Profile Parameters

We measured the C IV line shift, $FWHM$, EW , and the first and second line moments. We define the line shift, Δv , as the location of the line peak relative to 1549Å, in km s $^{-1}$. The location of 1549Å is determined from the redshifts listed on NED. We have checked the references for the redshifts to investigate how z was estimated, but not all of the references report this. For those that did specify, the redshifts were determined from the narrow emission lines (e.g., [O III] $\lambda 5007$).

IUE observations were done using a very large aperture, so the values of Δv for the IUE sources may be biased. However, there is no noticeable difference between Δv estimated from the IUE spectra, and those estimated from the HST spectra. Furthermore, the Δv parameter does not enter into our final analysis, and so even if the IUE Δv parameters are significantly biased our conclusions remain unchanged.

The first moment of the C IV line is the centroid, μ_{CIV} , and the square root of the second central moment is the line dispersion, σ_* . The zeroth line moment is the line flux. The line moments are calculated as

$$F = \sum_{i=1}^n y_i \delta \lambda \quad (13)$$

$$\mu_{CIV} = \frac{\sum_{i=1}^n x_i y_i}{\sum_{i=1}^n y_i} \quad (14)$$

$$\sigma_*^2 = \frac{\sum_{i=1}^n x_i^2 y_i}{\sum_{i=1}^n y_i} - \mu_{CIV}^2. \quad (15)$$

Here, F is the line flux, $\delta \lambda$ is the spacing between subsequent wavelengths, y is the observed spectral flux density, and x is the velocity relative to 1549Å. In practice we do not perform the sums over all the n data points, but rather only over those data points with $\hat{f}_i \geq 0.05(\max \hat{f})$, and assuming that the profile is monotonically decreasing blueward and redward of the peak. Here, \hat{f} denotes the best-fit line profile, found from modelling the emission lines as a sum of Gaussians. This allows us to define the extent of the line profile. Although this gives us biased measurements of the line moments, it keeps these measurements stable. In particular, σ_* can be very sensitive to the profile wings, which have the highest uncertainty. By truncating the line profile we keep the estimate stable and less sensitive to errors in the Fe and continuum subtraction, as well as errors in the He II $\lambda 1640$ and O III] $\lambda 1665$ subtraction.

The line moments are calculated using the observed line profile, y , and not the best-fit to the spectral flux densities, \hat{f} . We do this because the line moments are relatively insensitive to a lack of smoothness.

To be specific, consider a line profile, $f(x)$, and its Fourier transform, $\tilde{f}(k)$. For simplicity, we consider the continuous case here. The j^{th} unnormalized line moment, μ_j , may be written in terms of the Fourier transform of the line profile:

$$\mu_j = \int_{-\infty}^{\infty} x^j f(x) dx = \frac{\tilde{f}^{(j)}(0)}{(-2\pi i)^j}, \quad (16)$$

where $\tilde{f}^{(j)}(k)$ is the j^{th} derivative of $\tilde{f}(k)$ and $i = \sqrt{-1}$. One can see from Equation (16) that the line moments only depend on $\tilde{f}(k)$ near $k = 0$, and are thus insensitive to the high frequency behavior of $f(x)$. A generic smoothing operator, such as a Gaussian fit, will shrink the high k components of $\tilde{f}(k)$ more than the low k , as it is generally the case that the high k components have lower signal-to-noise. However, because the line moments do not depend on the high k components, nothing is gained by enforcing smoothness. Because of this we just use the observed C IV profile, y , as it is an unbiased estimate of the true profile, f , whereas the best-fit estimate, \hat{f} , is a biased estimate.

There has been some discussion in the literature over whether $FWHM$ or σ_* is the better width to use in estimating m (Fromerth & Melia 2000; Peterson et al. 2004). Fromerth & Melia (2000) suggested using the line dispersion, σ_* , arguing that it provides a better estimate of the velocity dispersion for an arbitrary line profile. Other advantages of σ_* include its insensitivity to noise and narrow absorption lines. However, σ_* can be significantly biased due to its sensitivity to blending with other lines in the line wings, and to the removal of continuum and iron emission. These facts can be understood in light of Equation (16), which shows that the second moment of the line depends on the low- k behavior. Because of this, σ_* is relatively unaffected by information on small scales, such as noise and narrow absorption lines, but is significantly affected by information on large scales, such as line blending, truncation of the line profile, and continuum placement. The $FWHM$, on the other hand, is insensitive to line blends and errors in the continuum and iron subtraction. In addition, $FWHM$ is easily measured, however it probably provides a poor estimate of the velocity dispersion for irregularly shaped lines profiles. Peterson et al. (2004) compared the strengths and weaknesses of these two measurements and concluded that σ_* was the better parameter when measured in the RMS spectrum.

In order to choose the better SES estimate of the BLR velocity dispersion, we calculate the partial correlation between m and $FWHM$ and σ_* , respectively. The partial correlation coefficient describes the correlation between m and line width at a given luminosity; the line width with the higher partial correlation should give a better estimate of m . The partial linear correlation between $\log FWHM$ and m is 0.36, while the partial linear correlation between $\log \sigma_*$ and m is 0.31. Because the $FWHM$ has a moderately higher partial correlation, and because the $FWHM$ is not as affected by errors in the line deblending, continuum placement, etc., we use the $FWHM$ as an estimate of the velocity dispersion throughout the rest of this analysis.

We only measure the $FWHM$ of the H β emission line. This is because we are only concerned with getting an estimate of M_{BH} from single-epoch H β based on the virial theorem for comparison with our C IV-based estimates, so the only line parameter of interest is the H β width.

The standard errors on the line parameter measurements are estimated using the bootstrap (Efron 1979). In this method, we take our best-fit line profile spectral flux densities, \hat{f} , and generate $n_{\text{boot}} = 128$ simulated observed line profiles by adding Gaussian noise to \hat{f} . We then estimate the line parameters of the simulated line profiles and calculate the variance in these parameters over the bootstrap samples.

In Figure 3 we plot $\log M_{BH}$ against $\log \lambda L_{\lambda}(1549 \text{ \AA})$, $\log FWHM$, $\log \sigma_*$, $\log EW$, Δv , μ_{CIV} , and continuum spectral slope. We report our measurements in Table 4. We have compared our measurements with

Wang et al. (1996), Bechtold et al. (2002), Baskin & Laor (2004), and Kuraszkiewicz et al. (2004), and find them to be consistent after accounting for the different procedures used to measure these quantities. For clarity, we have removed three outliers in α from the plot of m against α . These sources were 3C 390.3, NGC 3516, and NGC 7469. 3C 390.3 is a broad-line radio galaxy with highly variable Balmer lines and double-peaked H α (Corbett et al. 1998) and H β (Osterbrock et al. 1976) profiles; the C IV emission line also exhibits a double-peaked profile. The other two sources represent some of the faintest sources in our sample, and their spectra may have a contribution from their host galaxies; however, we notice nothing unusual about their spectra, save for their unusually soft values of α .

5. SELECTING THE IMPORTANT PARAMETERS

It is useful to investigate whether any of the additional parameters that we measured for C IV are significantly correlated with m , and thus contribute information about m in addition to that in l and $FWHM$. We used our sample of 25 sources with M_{BH} from reverberation mapping to test if including $\log EW$, α , μ_{CIV} , or Δv resulted in more accurate estimates of M_{BH} . However, we did not find any evidence to warrant the inclusion of these parameters.

In order to assess whether the data support including any additional parameters, we express m as a linear combination of all possible combinations of $\log \lambda L_\lambda$, $\log FWHM$, $\log EW$, α , μ_{CIV} , and Δv , a total of $2^6 = 64$ subsets. The regression coefficients are estimated via least-squares, and the result is a set of 64 linear regressions. In order to assess the relative merits of each of the regressions, and thus each of the respective parameters, we employ the Bayesian Information Criterion (*BIC* Schwartz 1979). Using the *BIC* allows us to undertake a Bayesian comparison of the models without actually carrying out the full Bayesian prescription, considerably simplifying things. The *BIC* is easily obtained from the log-likelihood of the data as

$$BIC = 2\ell(\hat{\psi}) + d \ln n. \quad (17)$$

Here, $\ell(\hat{\psi})$ is the log-likelihood of the data evaluated at the maximum-likelihood estimate, ψ denotes the regression parameters, d is the number of parameters in the regression, and n is the number of data points.

The only parameter significantly correlated with m is l , with a posterior probability of $p_l = 0.975$. The data are ambiguous as to whether $FWHM$ is related to M_{BH} ($p_{FWHM} = 0.562$); however, when using the *BIC* we did not compare with regressions that assume $M_{BH} \propto FWHM_{CIV}^2$, and we perform a more careful analysis in § 6.2. In addition, the data give weak evidence that the remaining parameters are unrelated to m . The posterior probabilities that m is correlated with these parameters are estimated to be 0.270, 0.210, 0.198, and 0.186 for $\log EW$, μ_{CIV} , Δv , and α , respectively.

6. REGRESSION ANALYSIS

Now that we have ruled out including any additional parameters for estimating M_{BH} from SES, we proceed to investigate the M_{BH} – L relationship and the C IV R – L relationship. Because $p(l|m)$ and $p(v|l, m)$ are statistically independent in their parameters, we can analyze each one separately. Throughout this section we will be using our sample of 25 sources with black hole mass measurements from reverberation mapping. We begin by investigating the M_{BH} – L relationship.

6.1. The M_{BH} - L Relationship

We fit a linear relationship of the form $l = \alpha_0 + \alpha_m m$, assuming that the scatter about this relationship is independent of m and z . Because we are fitting the distribution of l at a given m , we use the BCES($Y|X$) (Akritas & Bershady 1996) regression. The BCES methods take into account measurement errors in both coordinates by correcting their moments; however, the measurement errors are small compared to the variance in both m and l , so the correction is small. Based on the regression, we find

$$l = 35.72(\pm 1.67) + 1.17(\pm 0.22)m. \quad (18)$$

Here, $l = \log \lambda L_\lambda(1549\text{\AA})$. The empirical value of $\hat{\alpha}_m = 1.17 \pm 0.22$ is consistent with $L \propto M_{BH}$, if one assumes that $L_\lambda \propto L$. The intrinsic scatter in Equation (18) is estimated to be $\hat{\sigma}_l = 0.61$ dex. The residuals and their cumulative distribution function (CDF) are shown in Figure 4. A Kolmogorov-Smirnov test found that the regression residuals are not significantly different from a normal distribution, implying that $p(l|m)$ is normal with mean given by Equation (18) and standard deviation $\sigma_l \approx 0.61$ dex.

The value of $\hat{\alpha}_m$ found here is consistent with $M_{BH} \propto L^{0.9 \pm 0.15}$ found by Netzer (2003) and $M_{BH} \propto L^{0.97 \pm 0.16}$ found by Corbett et al. (2003). Peterson et al. (2004) used the 35 AGN with reverberation mapping data to estimate the M_{BH} - L relationship for L_λ at 5100\AA . Using the BCES bisector regression, they find $M_{BH} \propto L_{5100}^{0.79 \pm 0.09}$. This is shallower than our result of $M_{BH} \propto L_{1549}^{1.17 \pm 0.22}$, although the two logarithmic slopes are consistent within the errors. The difference in the two values most likely results from the different regressions used. We used the BCES($Y|X$) because we are modelling $p(l|m)$, where as the bisector slope gives the regression that bisects the distribution of l at a given m , and of m at a given l .

Woo & Urry (2002) did not find any evidence for a correlation between M_{BH} and the bolometric luminosity. They used both a sample of reverberation-mapped AGNs and Seyfert galaxies with black hole masses derived from the stellar velocity dispersion. In neither case did they find evidence for a correlation, in contrast to the results found here and by others. Unfortunately, Woo & Urry (2002) did not perform a regression analysis or report a correlation coefficient, so it is difficult to do a quantitative comparison of their results with ours.

We have found here that $\hat{\alpha}_m = 1.17 \pm 0.22$ for the Peterson et al. (2004) sample. However, these sources are all at low redshift and have $\dot{m} = 0.01$ – 1 (Woo & Urry 2002; Peterson et al. 2004), and thus this value of α_m may not be valid for sources with $\dot{m} \lesssim 0.01$ and $z \gtrsim 0.2$. Furthermore, most high z broad line quasars have luminosities and M_{BH} greater than that of the Peterson et al. (2004) sample, and it is possible that $\alpha_m \neq 1$ outside of the reverberation mapping sample range. It is also possible that the scatter about the M_{BH} - L relationship depends on z . The most likely source of a redshift dependence for ϵ_l is evolution of the distribution of \dot{m} (e.g., Haiman & Menou 2000; Merloni 2004; Hopkins et al. 2006; Steed & Weinberg 2006), and possibly evolution of the bolometric correction. The average \dot{m} has been observed to increase with increasing z (McLure & Dunlop 2004), but this is likely due to selection effects. Because of these issues, one should exhibit caution when applying this M_{BH} - L relationship to high z sources.

6.2. Inferring the C IV R - L Relationship

In this subsection, we investigate the C IV R - L relationship using the reverberation mapping sample. We perform a linear regression to fit for the value of θ_l , $R \propto L^{\theta_l}$, by noting that $M_{BH} \propto L^{\theta_l} V^2$. Based on the results obtained here, we find $M_{BH} \propto L_{1549}^{0.41 \pm 0.07} FWHM_{CIV}^2$, consistent with $M_{BH} \propto L_{1549}^{1/2} FWHM_{CIV}^2$ expected from simple photoionization theory.

To estimate θ_l , we fit a linear relationship of the form $2v = m - m_0^{BL} - \theta_l l$ using the BCES($Y|X$) method. Here, the free parameters are m_0^{BL} and θ_l . The result is

$$\hat{m}_{CIV} = -17.82(\pm 2.99) + 0.41(\pm 0.07)l + 2 \log FWHM_{CIV}. \quad (19)$$

The intrinsic scatter about this relationship is $\hat{\sigma}_{CIV} = 0.40$ dex, where we have corrected for the measurement errors in m and $FWHM_{CIV}$. The correlation between the regression coefficients is $Corr(\hat{m}_0^{CIV}, \hat{\theta}_l) = -0.9996$. The regression results are consistent with the expectation from simple photoionization theory, $R \propto L_{1549}^{1/2}$ (cf. Eq.[7]). A Kolmogorov-Smirnov test found that the regression residuals are not significantly different from a normal distribution.

Performing the regression with v as the dependent variable ensures that the M_{BH} - L relationship does not ‘absorb’ into the regression coefficients, as the regression models the distribution of v at a given l and m . However, if we had performed the regression by fitting the distribution of m as a function of l and v , the intrinsic correlation between m and l would have absorbed into the results. In this case we would be modelling $p(m|l, v)$, and the statistical model would be over-parameterized because we have only three variables. However, by separating $p(m|l, v)$ into $p(l|m)$ and $p(v|l, m)$, as was done in § 2.2, we can analyze each distribution separately and uniquely determine their parameters.

The residuals of the C IV broad line estimate, given by Equation (19), and their CDF are shown in Figure 5. In general, there is no obvious evidence for a violation of the regression assumptions. However, there appears to be a possible trend in the residuals with $FWHM$. To test this we calculated the linear correlation coefficient between the residuals and $\log FWHM$. This correlation was significant at only $\approx 1.7\sigma$. Therefore there is no significant evidence for a correlation in the residuals with $FWHM$, justifying the assumption $M_{BH} \propto L_{1549}^{\theta_l} FWHM^2$. Rank correlation tests gave similar results.

Very similar results were found by Vestergaard & Peterson (2006). However, our work differs from their’s in that Vestergaard & Peterson (2006) assumed that the C IV and H β BLRs have the same dependence on L_{UV} , $R \propto L_{UV}^{0.53}$, and only fit the constant term. In contrast, we fit both the constant term and the coefficient for the dependence of line width on luminosity.

One can use Equation (9) to combine the mass estimates based on the M_{BH} - L with the C IV broad line mass estimate. Combining the two relationships, and taking $\sigma(z) \rightarrow \infty$, we find

$$\mu = -30.53 + 0.54l + 1.40 \log FWHM. \quad (20)$$

The intrinsic uncertainty in μ is reduced to $\sigma_\mu \approx 0.33$ dex, an improvement of $\approx 18\%$ over the broad line mass estimates. However, as mentioned in § 6.1, there is considerable systematic uncertainty on the behavior of the M_{BH} - L relationship outside of the range probed by the reverberation mapping sample, and thus it may be safer to just use \hat{m}_{CIV} .

There has been some concern over the effectiveness of using the C IV emission line for estimating quasar black hole masses (Shemmer et al. 2004; Baskin & Laor 2005). If one ignores the C IV $FWHM$, and only uses the continuum luminosity to estimate M_{BH} , then the intrinsic scatter is $\sigma_l \approx 0.6$ dex (cf. § 6.1). However, the intrinsic uncertainty in an estimate of M_{BH} using the C IV R - L relationship and $FWHM$ is $\sigma_{CIV} \approx 0.4$ dex, a improvement over the M_{BH} - L relationship of $\sim 1/3$. This improvement is significant, and therefore we conclude that the C IV line may be used for estimating SMBH masses.

We can estimate σ_v^2 by comparing the C IV $FWHM$ for the RMS spectrum with that obtained from a single-epoch spectrum. To do this we use the sources from Peterson et al. (2004) with C IV $FWHM$

measured from the RMS spectrum, $FWHM_{RMS}$, excluding Fairall 9. We omitted Fairall 9 because its $FWHM_{RMS}$ was considered to be unreliable by Peterson et al. (2004). The remaining five data points are consistent with a 1:1 relationship between $FWHM_{RMS}$ and $FWHM_{SE}$. Estimating the intrinsic scatter using these five data points is difficult, particularly because the measurement errors are large. In fact, the observed scatter about $FWHM_{RMS} = FWHM_{SE}$ is consistent with entirely being the result of the measurement errors. This suggests that σ_v is small, and it is likely that $\sigma_v \lesssim 0.1$ dex.

If we assume that the only sources for scatter in the broad line estimates of m are from the $R-L$ relationship and from using the single-epoch line width to estimate V , then a value of $\sigma_v \approx 0.1$ dex implies that the intrinsic scatter about the $R-L$ relationship for C IV is $\hat{\sigma}_r \approx 0.35$ dex. This is about a factor of two larger than the value $\hat{\sigma}_r \approx 0.18$ dex found for H β by Peterson et al. (2004), where we have converted the value $\hat{\sigma}_r \approx 40\%$ to dex. This larger scatter in the C IV $R-L$ relationship implies that the H β mass estimates are more efficient than the C IV ones. However, Vestergaard & Peterson (2006) found that the H β mass estimates have a statistical scatter of $\hat{\sigma}_{H\beta} \approx 0.43$ dex, and thus are just as accurate as the C IV-based ones. This larger value of $\sigma_{H\beta}$ implies that either there is significant uncertainty in using the SES H β line width to estimate the BLR velocity dispersion, $\sigma_v^{H\beta} \approx 0.36$, or that there are additional sources of uncertainty in the broad line mass estimates beyond the scatter in the $R-L$ relationship and the uncertainty in using the SES line width instead of the variable component line width. If there are additional sources of scatter in the SES mass estimates, then $\hat{\sigma}_r \approx 0.35$ dex represents an upper bound on the C IV $R-L$ relationship scatter.

Equation (7) implies that the scatter in the $R-L$ relationship is the result of variations in the BLR ionization parameter, gas density, and average ionizing photon energy. While there are likely other sources of scatter in the $R-L$ relationship, such as inclination, variability, and conversion between L_λ and L_{ion} , differences in BLR properties certainly contribute to this scatter and possibly dominate it. The fact that $\sigma_r^{CIV} \lesssim 1.6\sigma_r^{H\beta}$ suggests that the magnitude of the dispersion in these properties is larger for the C IV emitting region. In addition, the regressions of (Peterson et al. 2004) are consistent with $R_{H\beta} \propto L_{1450}^{1/2}$, similar to the result found here and by Vestergaard & Peterson (2006) for C IV.

7. COMPARING THE H β - AND C IV-BASED MASS ESTIMATES

It is worth comparing our estimates of m based on single-epoch C IV to those based on combining single-epoch H β with the $R_{H\beta}-L$ relationship. To do this, we took our sample of 100 sources that have data for both C IV and H β and calculated estimates of m from each. We compare the mass estimates obtained from both emission lines, and find that the two give mass estimates that are consistent so long as one uses the UV continuum to estimate the BLR size.

For the H β emission line, we estimate the BLR size from both the optical and UV $R_{H\beta}-L$ relationships. The BLR size, $R_{H\beta}$, is estimated as

$$\frac{R_{H\beta}}{10 \text{ lt} - \text{dy}} = R_0 \left(\frac{\lambda L_\lambda}{10^{44} \text{ ergs s}^{-1}} \right)^\alpha. \quad (21)$$

For R_0 and α in the optical $R_{H\beta}-L$ relationship, we use the luminosity at 5100\AA and the average of the BCES bisector and FITEXY (Press et al. 1992) fits of Kaspi et al. (2005), $(\hat{R}_0, \hat{\alpha}) = (2.23 \pm 0.21, 0.69 \pm 0.05)$. For the UV $R_{H\beta}-L$ relationship, we use the luminosity at 1450\AA and $(R_0, \alpha) = (2.38, 0.5)$. We assume $R_{H\beta} \propto L_{1450}^{1/2}$ to allow more direct comparison with the C IV-based mass estimates, and because the fits of Kaspi et al. (2005) are consistent with this form. Using the averaged values of R for the Balmer lines as listed by Kaspi et al. (2005), we recalculated the $R-L_{1450}$ relationship for H β with α fixed at $\alpha = 0.5$, and found

$R_0 = 2.38 \pm 0.25$. We then use $R_{H\beta}$ with $H\beta$ $FWHM$ to calculate $m_{H\beta}$ from Equation (1), after converting the $H\beta$ $FWHM$ to a velocity dispersion assuming $FWHM/V = 2$, based on the average $FWHM/\sigma_*$ from Peterson et al. (2004).

Based on the results of § 6.2, we calculate estimates of M_{BH} from the C IV line for these sources as $\hat{m}_{CIV} = -21.92 + 0.5l_{1549} + 2v_{CIV}$. This form was found using the same method as described in § 6.2, but with θ_l fixed at $\theta_l = 1/2$. In Table 5 we report the broad line mass estimates based on the $H\beta$ and C IV lines for these sources, as well as a weighted average of the two.

In Figure 6 we show $\hat{m}_{H\beta}$ vs \hat{m}_{CIV} for both the optical and UV $R_{H\beta}-L$ relationship. We also show the 99% (2.6σ) confidence region for the parameters of a BCES bisector fit to $\hat{m}_{CIV} = A + B\hat{m}_{H\beta}$. As can be seen, the values of $\hat{m}_{H\beta}$ calculated using the UV $R_{H\beta}-L$ relationship are more consistent with the C IV-based ones. In addition, a pure 1:1 relationship falls outside of the 99% confidence region on the BCES bisector parameters for the optical-based $\hat{m}_{H\beta}$ values, but it is contained within the 99% confidence region for the UV-based estimates. In fact, the BCES bisector fit for the UV-based mass estimates differs from a 1:1 relationship at a significance level of only 1.9σ . Our results are in agreement with Warner et al. (2003) and Dietrich & Hamann (2004), who also compared the C IV- and $H\beta$ -based mass estimates and found them to be consistent.

That the C IV- and $H\beta$ -based mass estimates are consistent is in contrast to the conclusions of Baskin & Laor (2005) and Shemmer et al. (2004). Baskin & Laor (2005) suggested that C IV-based mass estimates may be problematic because they find that $\log(FWHM_{CIV}/FWHM_{H\beta})$ is significantly anti-correlated with $\log FWHM_{H\beta}$. However this is expected even when $v_{H\beta} \propto v_{CIV}$, as an anti-correlation between the ratio of the line widths and the $H\beta$ $FWHM$ is expected by construction; i.e., an anti-correlation between $\log FWHM_{CIV} - \log FWHM_{H\beta}$ and $\log FWHM_{H\beta}$ is expected so long as the deviations of $\log FWHM_{CIV}$ and $\log FWHM_{H\beta}$ from their respective means are not strongly correlated. In addition, none of the sources in the Baskin & Laor (2005) sample have $H\beta$ broader than C IV for $FWHM_{H\beta} < 4000 \text{ km s}^{-1}$. To a lesser extent, a similar effect is seen in Figure 7 of Shemmer et al. (2004) and Figure 4 of Warner et al. (2003). In Figure 6 we compare the C IV and $H\beta$ $FWHM$ for our sources. We find that most of the sources with $FWHM_{H\beta} \lesssim 2000 \text{ km s}^{-1}$ tend to have broader C IV lines. While the line widths certainly do not have a 1:1 relationship, the BCES bisector fit found that on average $FWHM_{H\beta}$ is approximately proportional to $FWHM_{CIV}$, $FWHM_{CIV} \propto FWHM_{H\beta}^{0.79 \pm 0.06}$. Baskin & Laor (2005) and Shemmer et al. (2004) did not perform a regression analysis, so we are unable to make a more quantitative comparison.

If the line widths are set by the virial relationship, we would expect $FWHM_{CIV} \propto FWHM_{H\beta}$. While the divergence from $FWHM_{CIV} \propto FWHM_{H\beta}$ is likely real (3.5σ significance), it is small, especially when compared with the intrinsic scatter in the $FWHM$ plot. Furthermore, this divergence from $FWHM_{CIV} \propto FWHM_{H\beta}$ does not appear to have a significant effect on the C IV mass estimates, as the masses inferred from the two emission lines differ only at the level of 1.9σ . As can be seen from the plot in Figure 6, any systematic difference between the C IV- and $H\beta$ -based mass estimates is small compared to the statistical scatter in \hat{m} .

Vestergaard & Peterson (2006) performed a reanalysis of the Baskin & Laor (2005) sample and concluded that the poor correlation between the C IV $FWHM$ and the $H\beta$ $FWHM$ seen by Baskin & Laor (2005) was due to the inclusion of a large number of Narrow Line Seyfert 1s (NLS1) and the subtraction of a C IV narrow component. Vestergaard (2004) noted that for these sources the C IV line profile is unlikely to be suitable for estimating M_{BH} , as there may be a strong component from an outflowing wind. Upon removing the NLS1s and the sources with poor IUE data, Vestergaard & Peterson (2006) found the correlation between

C IV *FWHM* and H β *FWHM* to be significantly better.

In addition, Baskin & Laor (2005) compared the correlation of C IV *EW* with $L/L_{edd} \propto L/M_{BH}$. A similar investigation was performed by Shemmer et al. (2004), where they compared the metallicity indicator N V/C IV with L/L_{edd} . Both authors found a stronger correlation when M_{BH} was estimated from the H β line as compared to C IV, and suggested that the C IV line may give a less efficient and possibly biased estimate of M_{BH} . However, as noted in § 2.3, correlation coefficients inferred from the estimated black hole masses must be interpreted with caution. In particular, the SES estimate of m , \hat{m} , merely defines the centroid of the probability density of $m|l, v, z$, and is in general *not* the actual m for an object. Therefore, this difference in the correlation coefficient between the H β - and C IV-based mass estimates may be just the result of random sampling, and it is unclear whether one can say that the correlation coefficients inferred from the two different mass estimates are inconsistent with those mass estimates being drawn from the same parent distribution.

The most direct test of the effectiveness of using C IV to estimate M_{BH} is found by comparing those values of \hat{m} estimated using C IV with the actual reverberation mapping values of m . This was done in § 6.2, where inclusion of the C IV *FWHM* resulted in a reduction of the error in \hat{m} of $\sim 1/3$. In addition, Figure 5 compares the C IV-based estimate of m with the reverberation mapping values. As can be seen, assuming $M_{BH} \propto FWHM_{CIV}^2$ is consistent with the reverberation mapping sample, and therefore there is no reason to assume that the C IV line gives a biased estimate of M_{BH} . If \hat{m}_{CIV} does give a biased estimate of m , then this bias is likely negligible compared to the variance in \hat{m}_{CIV} .

8. SUMMARY

In this work we have undertaken a statistical investigation of the best method to estimate SMBH mass based on the single-epoch C IV line and AGN continuum at 1549Å. The main conclusions are :

1. Estimating AGN black hole masses from a single-epoch spectrum is a considerably different problem than in the reverberation-mapping case. Because of this, one is not estimating M_{BH} directly, but calculating a probability distribution of M_{BH} given the observed luminosity, line width, and redshift, $p(m|l, v, z) \propto p(v|l, m, z)p(l|m, z)p(m|z)$.
2. Combining the information in L from both an intrinsic M_{BH} - L correlation and the R - L relationship results in improved black hole mass estimates. However, because of the current systematic uncertainties in the M_{BH} - L relationship, estimates based on its inclusion should be viewed with caution. In addition, incorporating information from the intrinsic distribution of M_{BH} also results in more accurate estimates, on average.
3. The distribution of M_{BH} inferred from the broad line mass estimates, \hat{m}_{BL} , is broader than the intrinsic distribution of M_{BH} , as \hat{m}_{BL} are estimates of m contaminated by ‘measurement error.’ In addition, it is necessary to estimate or assume $p(l|m, z)$ in order to estimate a survey’s completeness in M_{BH} .
4. The best estimates of M_{BH} based on the C IV emission line are obtained using the UV continuum luminosity and *FWHM*. We find evidence that the C IV line shift, centroid, *EW*, and spectral slope of the UV continuum do not contribute any additional information to estimating M_{BH} for a given L_{1549} and $FWHM_{CIV}$.

5. Using the reverberation mapping sample, we find an M_{BH} - L relationship of the form

$$l = 35.72(\pm 1.67) + 1.17(\pm 0.22)m. \quad (22)$$

The intrinsic scatter about this relationship is $\sigma_l \approx 0.61$ dex. Combining mass estimates based on this relationship with the broad line mass estimates results in a reduction in the statistical error of $\approx 18\%$.

6. We estimate a C IV R - L relationship of the form $R \propto L_{1549}^{0.41 \pm 0.07}$. This is consistent with an R - L relationship of the form $R \propto L^{1/2}$ predicted from simple photoionization physics or if the BLR size is set by the dust sublimation radius. The scatter about the C IV R - L relationship inferred from the reverberation mapping estimates of M_{BH} is $\sigma_r \approx 0.35$ dex.
7. A broad line estimate of m based on the C IV emission line may be calculated as

$$\log \hat{M}_{BH}/M_{\odot} = \hat{m}_{CIV} = -17.82(\pm 2.99) + 0.41(\pm 0.07) \log \lambda L_{\lambda}(1549\text{\AA}) + 2 \log FWHM_{CIV}. \quad (23)$$

Here, λL_{λ} is in units of ergs s^{-1} and $FWHM$ is in units of km s^{-1} . The correlation between regression coefficients is $Corr(\hat{m}_0^{CIV}, \hat{\theta}_l) = -0.9996$. The intrinsic scatter in m about Equation (23) is ≈ 0.40 dex.

8. The C IV- and $H\beta$ -based mass estimates are consistent if one assumes $R \propto L_{UV}^{1/2}$ for both emission lines. The two emission lines give estimates of M_{BH} with comparable accuracy.
9. We find evidence that the R - L relationships for C IV and $H\beta$ are similar in their dependence on L_{UV} . For both, $R \propto L_{UV}^{1/2}$ is consistent with the available data. Also, the scatter in the C IV R - L relationship is a factor $\lesssim 1.6$ larger. This suggests that the C IV broad line region gas has a larger dispersion in its properties (e.g., density, ionization parameter, inclination) than the $H\beta$ BLR gas.

We are grateful to Marianne Vestergaard for providing the UV Fe emission template used in this study, Jun Cui for directly obtaining the spectra for Q 1230+0947, and Marianne Vestergaard, Xiaohui Fan, Fulvio Melia, and Aneta Siemiginowska for stimulating discussions and helpful comments on an earlier version of this manuscript. We are also grateful to the referee for a careful reading of this work and helpful comments that contributed to the significant improvement of this paper. This research was supported in part by NASA/Chandra grant G04-5112X. This paper includes data gathered with the 6.5 meter Magellan Telescopes located at Las Campanas Observatory, Chile.

This research has made use of the NASA/IPAC Extragalactic Database (NED) which is operated by the Jet Propulsion Laboratory, California Institute of Technology, under contract with the National Aeronautics and Space Administration.

Funding for the SDSS and SDSS-II has been provided by the Alfred P. Sloan Foundation, the Participating Institutions, the National Science Foundation, the U.S. Department of Energy, the National Aeronautics and Space Administration, the Japanese Monbukagakusho, the Max Planck Society, and the Higher Education Funding Council for England. The SDSS Web Site is <http://www.sdss.org/>.

The SDSS is managed by the Astrophysical Research Consortium for the Participating Institutions. The Participating Institutions are the American Museum of Natural History, Astrophysical Institute Potsdam, University of Basel, Cambridge University, Case Western Reserve University, University of Chicago, Drexel University, Fermilab, the Institute for Advanced Study, the Japan Participation Group, Johns Hopkins University, the Joint Institute for Nuclear Astrophysics, the Kavli Institute for Particle Astrophysics

and Cosmology, the Korean Scientist Group, the Chinese Academy of Sciences (LAMOST), Los Alamos National Laboratory, the Max-Planck-Institute for Astronomy (MPIA), the Max-Planck-Institute for Astrophysics (MPA), New Mexico State University, Ohio State University, University of Pittsburgh, University of Portsmouth, Princeton University, the United States Naval Observatory, and the University of Washington.

REFERENCES

- Abazajian, K., et al. 2004, *AJ*, 128, 502
- Adams, F. C., Graff, D. S., & Richstone, D. O. 2001, *ApJ*, 551, L31
- Akritas, M. G., & Bershad, M. A. 1996, *ApJ*, 470, 706
- Baskin, A., & Laor, A. 2004, *MNRAS*, 350, L31
- Baskin, A., & Laor, A. 2005, *MNRAS*, 356, 1029
- Bechtold, J., Dobrzycki, A., Wilden, B., Morita, M., Scott, J., Dobrzycka, D., Tran, K., & Aldcroft, T. L. 2002, *ApJS*, 140, 143
- Bechtold, J., et al. 2003, *ApJ*, 588, 119
- Blandford, R. D., & McKee, C. F. 1982, *ApJ*, 255, 419
- Boroson, T. A., & Green, R. F. 1992, *ApJS*, 80, 109
- Cao, X., & Xu, Y. 2006, submitted to *ApJ*(astro-ph/0504662)
- Cardelli, J. A., Clayton, G. C., & Mathis, J. S. 1989, *ApJ*, 345, 245
- Collin, S., Boisson, C., Mouchet, M., Dumont, A.-M., Coupé, S., Porquet, D., & Rokaki, E. 2002, *A&A*, 388, 771
- Corbett, E. A., Robinson, A., Axon, D. J., Young, S., & Hough, J. H. 1998, *MNRAS*, 296, 721
- Corbett, E. A., et al. 2003, *MNRAS*, 343, 705
- Czerny, B., Rózańska, A., & Kuraszkiewicz, J. 2004, *A&A*, 428, 39
- Dietrich, M., Appenzeller, I., Vestergaard, M., & Wagner, S. J. 2002, *ApJ*, 564, 581
- Dietrich, M., & Hamann, F. 2004, *ApJ*, 611, 761
- Di Matteo, T., Springel, V., & Hernquist, L. 2005, *Nature*, 433, 604
- Done, C., & Krolik, J. H. 1996, *ApJ*, 463, 144
- Dunlop, J. S., McLure, R. J., Kucula, M. J., Baum, S. A., O’Dea, C. P., & Hughes, D. H. 2003, *MNRAS*, 340, 1095
- Efron, B. 1979, *Ann. Statist.*, 7, 1
- Evans, I. N., & Koratkar, A. P. 2004, *ApJS*, 150, 73
- Ferrarese, L., Pogge, R. W., Peterson, B. M., Merritt, D., Wandel, A., & Joseph, C. L. 2001, *ApJ*, 555, L79
- Fox, J. 1997, *Applied Regression Analysis, Linear Models, and Related Methods* (Thousand Oaks:Sage Publications, Inc.)
- Fromerth, M. J., & Melia, F. 2000, *ApJ*, 533, 172
- Gebhardt, K., et al. 2000, *ApJ*, 539, L13

- Gebhardt, K., et al. 2000, *ApJ*, 543, L5
- Gelman, A., Carlin, J. B., Stern, H. S., & Rubin, D. B. 2004, *Bayesian Data Analysis* (2nd ed.; Boca Raton:Chapman & Hall/CRC)
- Green, R. F., Schmidt, M., & Liebert, J. 1986, *ApJS*, 61, 305
- Haehnelt, M. G., & Kauffmann, G. 2000, *MNRAS*, 318, L35
- Haiman, Z., & Menou, K. 2000, *ApJ*, 531, 42
- Ho, L. C. 2002, *ApJ*, 564, 120
- Hopkins, P. F., Hernquist, L., Cox, T. J., Di Matteo, T., Robertson, B., & Springel, V. 2006, *ApJS*, 163, 1
- Hopkins, P. F., Narayan, R., & Hernquist, L. 2006, *ApJ*, 643, 641
- Jester, S. 2005, *ApJ*, 625, 667
- Kaspi, S., Smith, P. S., Netzer, H., Maoz, D., Jannuzi, B. T., & Giveon, U. 2000, *ApJ*, 533, 631
- Kaspi, S., Maoz, D., Netzer, H., Peterson, B. M., Vestergaard, M., & Jannuzi, B. T. 2005, *ApJ*, 629, 61
- Kormendy, J., & Richstone, D. 1995, *ARA&A*, 33, 581
- Krolik, J. H. 2001, *ApJ*, 551, 72
- Kukula, M. J., Dunlop, J. S., McLure, R. J., Miller, L., Percival, W. J., Baum, S. A., & O’Dea, C. P. 2001, *MNRAS*, 326, 1533
- Kuraszkiewicz, J. K., Green, P. J., Crenshaw, D. M., Dunn, J., Forster, K., Vestergaard, M., & Aldcroft, T. L. 2004, *ApJS*, 150, 165
- Magorrian, J., et al. 1998, *AJ*, 115, 2285
- Marchesini, D., Celotti, A., & Ferrarese, L. 2004, *MNRAS*, 351, 733
- Marconi, A., & Hunt, L. K. 2003, *ApJ*, 589, L21
- Marziani, P., Sulentic, J. W., Zamanov, R., Calvani, M., Dultzin-Hacyan, D., Bachev, R., & Zwitter, T. 2003, *ApJS*, 145, 199
- McIntosh, D. H., Rieke, M. J., Rix, H.-W., Foltz, C. B., & Weymann, R. J. 1999, *ApJ*, 514, 40
- McLeod, K. K., & McLeod, B. A. 2001, *ApJ*, 546, 782
- McLure, R. J., Kukula, M. J., Dunlop, J. S., Baum, S. A., O’Dea, C. P., & Hughes, D. H. 1999, *MNRAS*, 308, 377
- McLure, R. J., & Dunlop, J. S. 2001, *MNRAS*, 327, 199
- McLure, R. J., & Dunlop, J. S. 2002, *MNRAS*, 331, 795
- McLure, R. J., & Jarvis, M. J. 2002, *MNRAS*, 337, 109
- McLure, R. J., & Dunlop, J. S. 2004, *MNRAS*, 352, 1390

- McLure, R. J., & Jarvis, M. J. 2004, MNRAS, 353, L45
- Merloni, A. 2004, MNRAS, 353, 1035
- Merloni, A., Heinz, S., & di Matteo, T. 2003, MNRAS, 345, 1057
- Merritt, D., & Ferrarese, L. 2001, ApJ, 547, 140
- Merritt, D., & Poon, M. Y. 2004, ApJ, 606, 788
- Nelson, C. H., Green, R. F., Bower, G., Gebhardt, K., & Weistrop, D. 2004, ApJ, 615, 652
- Netzer, H. 1990, in Active Galactic Nuclei, ed. R. D. Blandford, H. Netzer, & L. Woltjer (Berlin:Springer), 137
- Netzer, H., & Laor, A. 1993, ApJ, 404, L51
- Netzer, H. 2003, ApJ, 583, L5
- Nicastro, F., Martocchia, A., & Matt, G. 2003, ApJ, 589, L13
- Nolan, L. A., Dunlop, J. S., Kukula, M. J., Hughes, D. H., Boroson, T., & Jimenez, R. 2001, MNRAS, 323, 308
- Oke, J. B., & Gunn, J. E. 1983, ApJ, 266, 713
- O'Neill, P. M., Nandra, K., Papadakis, I. E., & Turner, T. J. 2005, MNRAS, 358, 1405
- Onken, C. A., Ferrarese, L., Merritt, D., Peterson, B. M., Pogge, R. W., Vestergaard, M., & Wandel, A. 2004, ApJ, 615, 645
- Osterbrock, D. E., Koski, A. T., & Phillips, M. M. 1976, ApJ, 206, 898
- Percival, W. J., Miller, L., McLure, R. J., & Dunlop, J. S. 2001, MNRAS, 322, 843
- Pessah, M, 2006, submitted to ApJ(astro-ph/0509358)
- Peterson, B. M. 1993, PASP, 105, 247
- Peterson, B. M., et al. 2004, ApJ, 613, 682
- Peterson, B. M., et al. 2005, ApJ, 632, 799
- Press, W. H., Teukolsky, S. A., Vetterling, W. T., & Flannery, B. P. 1992, Numerical Recipes (Second ed.; Cambridge:Cambridge Univ. Press), 660
- Richards, G. T., et al. 2001, AJ, 121, 2308
- Richards, G. T., Vanden Berk, D. E., Reichard, T. A., Hall, P. B., Schneider, D. P., SubbaRao, M., Thakar, A. R., & York, D. G. 2002, AJ, 124, 1
- Schlegel, D. J., Finkbeiner, D. P., & Davis, M. 1998, ApJ, 500, 525
- Schwartz, G. 1979, Ann. Statist., 6, 461
- Scott, J., Bechtold, J., Dobrzycki, A., & Kulkarni, V. P. 2000, ApJS, 130, 67

- Shemmer, O., Netzer, H., Maiolino, R., Oliva, E., Croom, S., Corbett, E., & di Fabrizio, L. 2004, *ApJ*, 614, 547
- Shields, G. A., Gebhardt, K., Salviander, S., Wills, B. J., Xie, B., Brotherton, M. S., Yuan, J., & Dietrich, M. 2003, *ApJ*, 583, 124
- Silk, J., & Rees, M. J. 1998, *A&A*, 331, L1
- Spergel, D. N., et al. 2003, *ApJS*, 148, 175
- Steed, A., & Weinberg, D. H. 2006, submitted to *ApJ*(astro-ph/0311312)
- Tremaine, S., et al. 2002, *ApJ*, 574, 740
- Véron-Cetty, M.-P., Joly, M., & Véron, P. 2004, *A&A*, 417, 515
- Vestergaard, M., & Wilkes, B. J. 2001, *ApJS*, 134, 1
- Vestergaard, M. 2002, *ApJ*, 571, 733
- Vestergaard, M. 2004, *ApJ*, 601, 676
- Vestergaard, M., & Peterson, B. M. 2006, *ApJ*, 641, 689
- Wandel, A., Peterson, B. M., & Malkan, M. A. 1999, *ApJ*, 526, 579
- Wang, T.-G., Zhou, Y.-Y., & Gao, A.-S. 1996, *ApJ*, 457, 111
- Wang, J.-M., Chen, Y.-M., & Zhang, F. 2006, *ApJ*, 647, L17
- Warner, C., Hamann, F., & Dietrich, M. 2003, *ApJ*, 596, 72
- Woo, J., & Urry, C. M. 2002, *ApJ*, 579, 530
- Wu, X.-B., Wang, R., Kong, M. Z., Liu, F. K., & Han, J. L. 2004, *A&A*, 424, 793
- Xie, G.-Z., Chen, L.-E., Li, H.-Z., Mao, L.-S., Dai, H., Xie, Z.-H., Ma, L., & Zhou, S.-B. 2005, *Chinese Journal of Astronomy and Astrophysics*, 5, 463

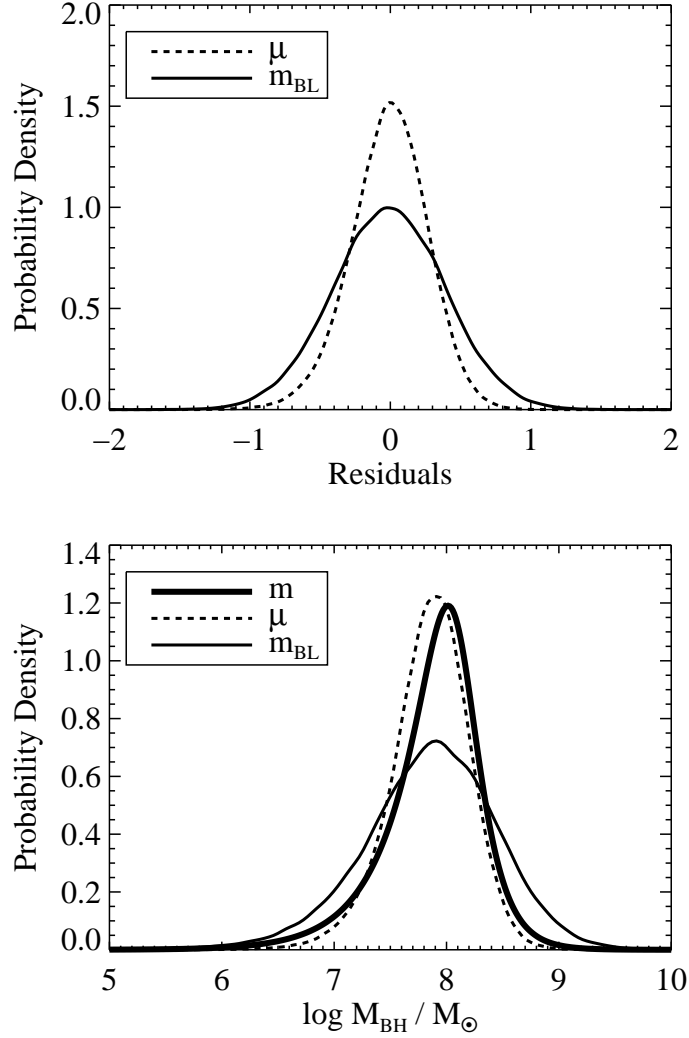


Fig. 1.— Results of the simulations described in § 2.2, illustrating the effectiveness of the mass estimate, μ , that combines the broad line mass estimates with the distribution of luminosities at a given black hole mass and the intrinsic distribution of M_{BH} . The upper panel shows the distribution of the residuals when using μ (dashed line) and the broad line mass estimate, \hat{m}_{BL} (solid line). The bottom panel compares the intrinsic distribution of m (thick solid line) with that inferred from the distribution of μ (dashed line) and \hat{m}_{BL} (thin solid line).

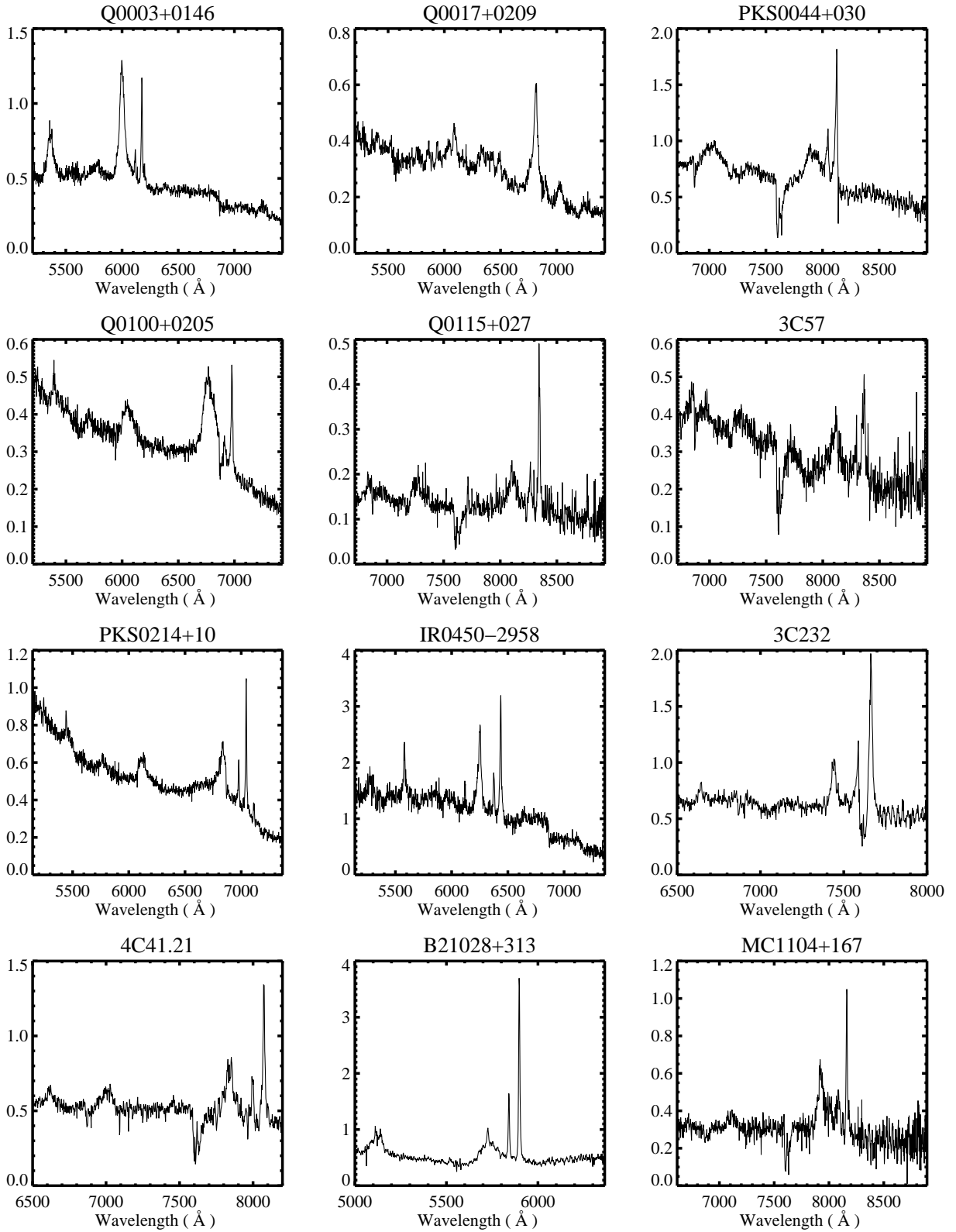


Fig. 2a.— New optical spectra, shown in the observed frame. The fluxes are in units of $10^{-15} \text{ ergs cm}^{-2} \text{ sec}^{-1} \text{ \AA}^{-1}$. The absorption features at $\sim 6875 \text{ \AA}$ and $\sim 7600 \text{ \AA}$ are the A- and B-band atmospheric absorption lines. Note the strong iron emission in Q1340-0038.

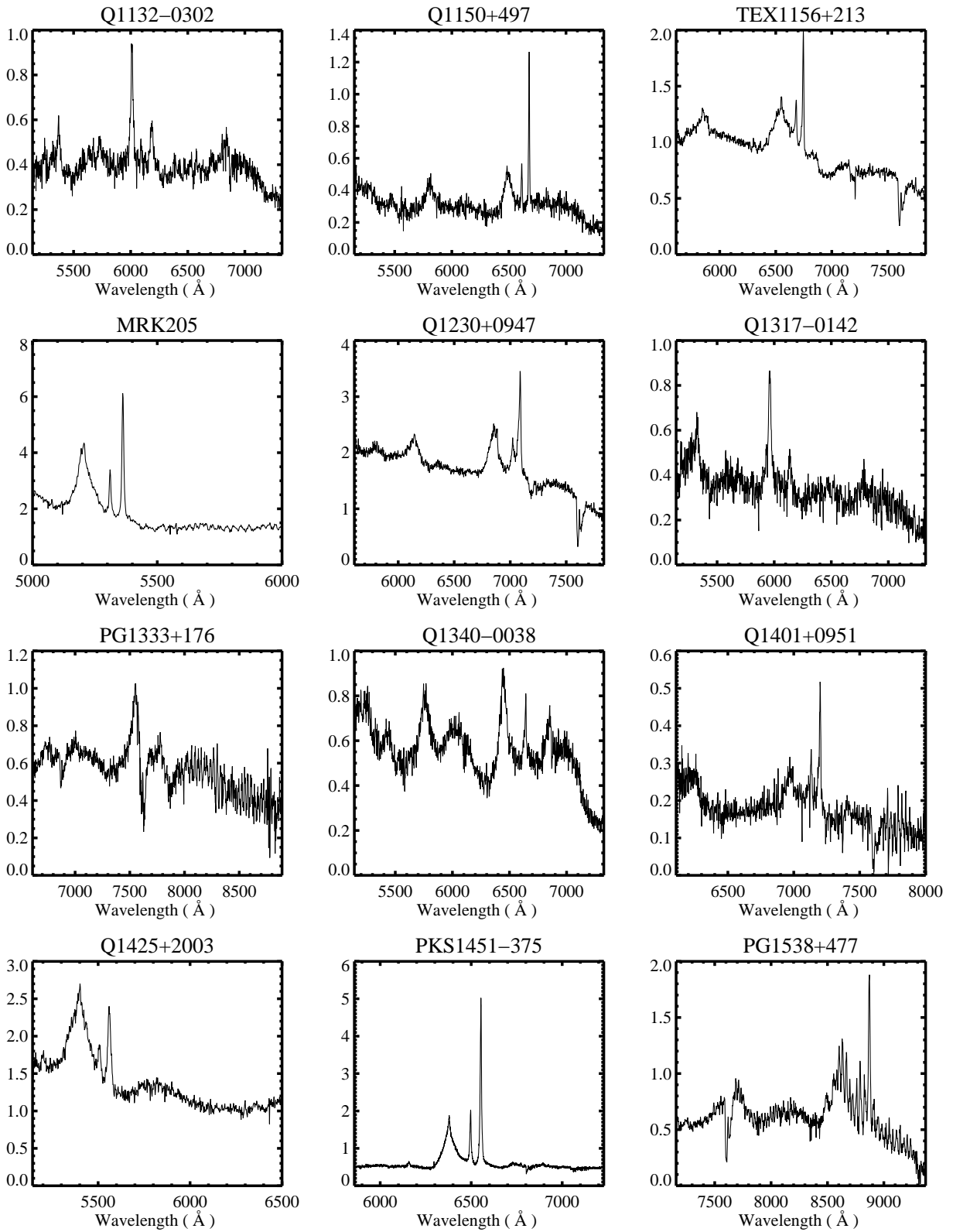


Fig. 2b.—

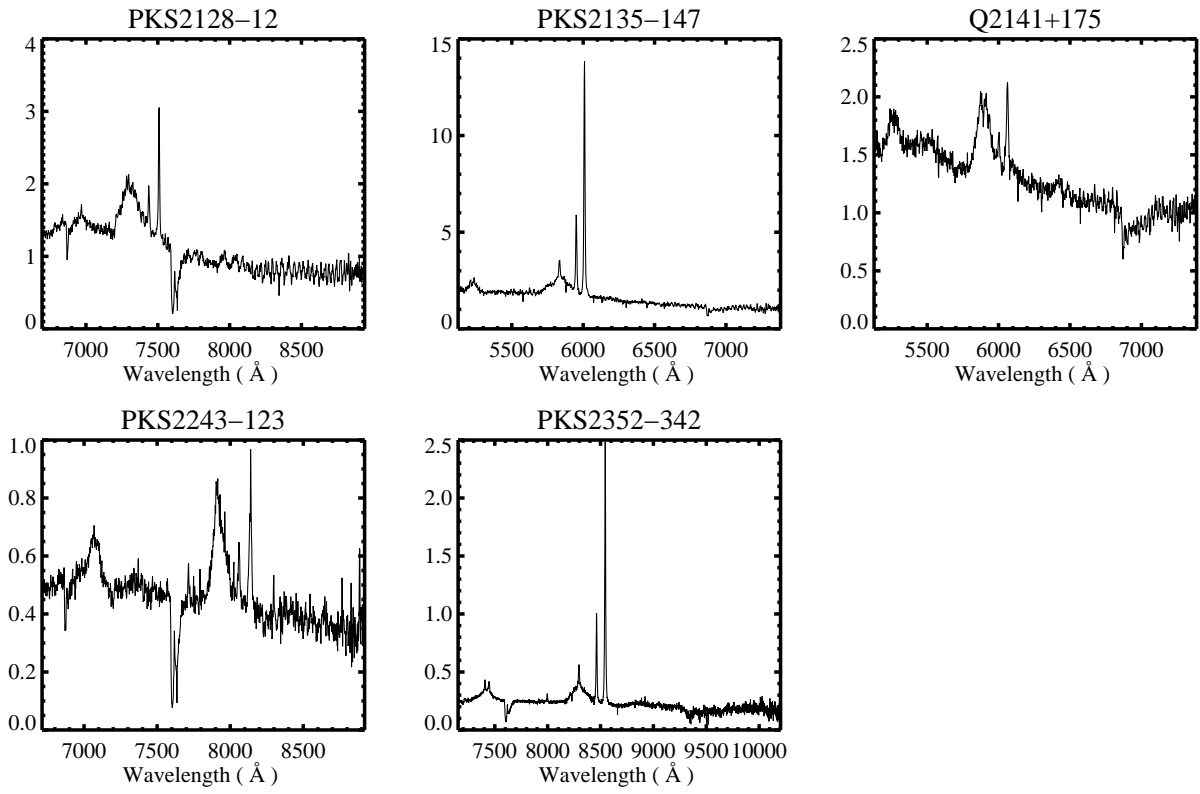


Fig. 2c.—

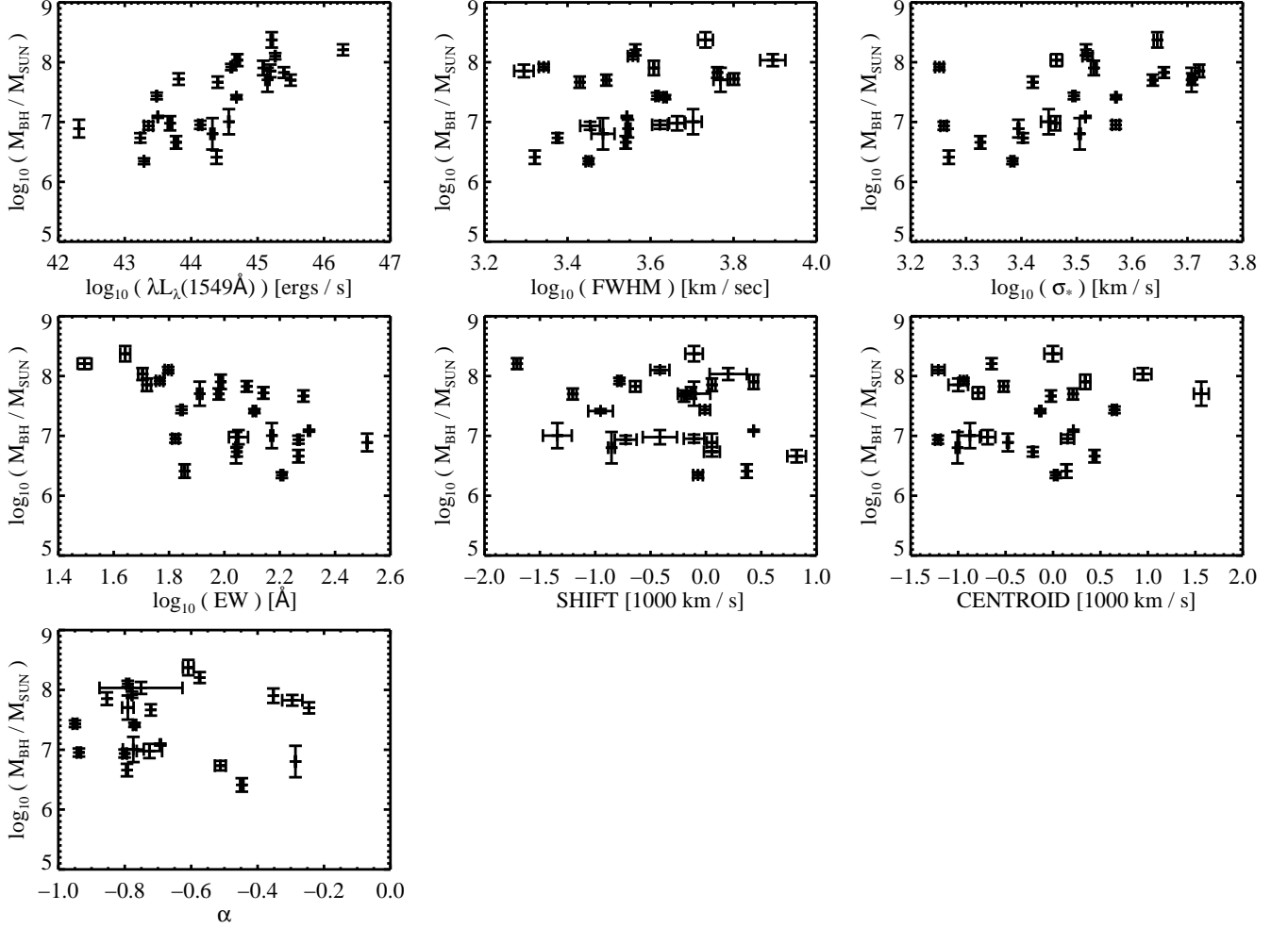


Fig. 3.— Plots showing m as a function of the measured quantities for the sample with reverberation mapping data. Three outliers in the m vs α plot have been removed so as to make the structure in the plot easier to see.

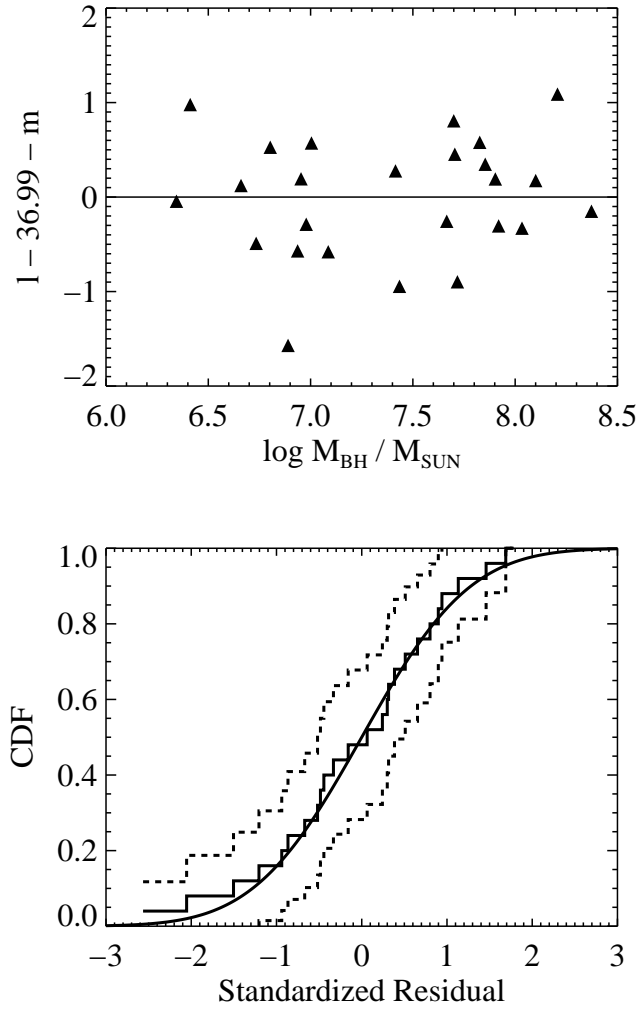


Fig. 4.— The residuals $l - \hat{l}$ as a function of m for the $M_{\text{BH}}-L$ relationship and the empirical CDF of the standardized residuals, $(l - \hat{l})/\hat{\sigma}_l$. The dashed lines define the 95% pointwise confidence interval of the empirical CDF, and the smooth solid line is the CDF of the standard normal density.

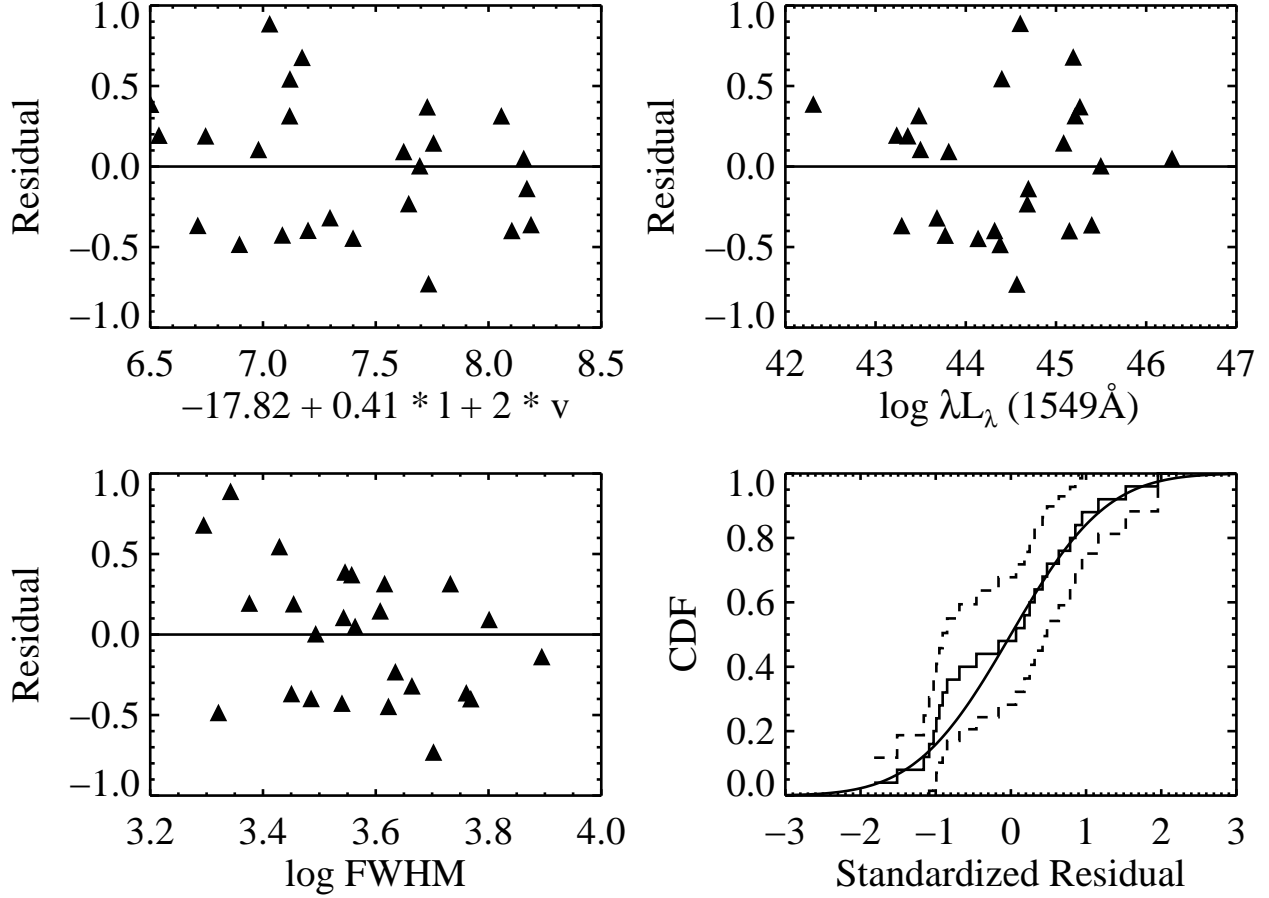


Fig. 5.— The residuals $m - \hat{m}_{CIV}$ for the C IV broad line mass estimate, shown as a function of \hat{m}_{CIV}, l , and $FWHM$. Also shown is the empirical CDF of the standardized residuals, $(m - \hat{m}_{CIV})/\hat{\sigma}_{CIV}$. The dashed lines define the 95% pointwise confidence interval of the empirical CDF, and the smooth solid line is the CDF of the standard normal density.

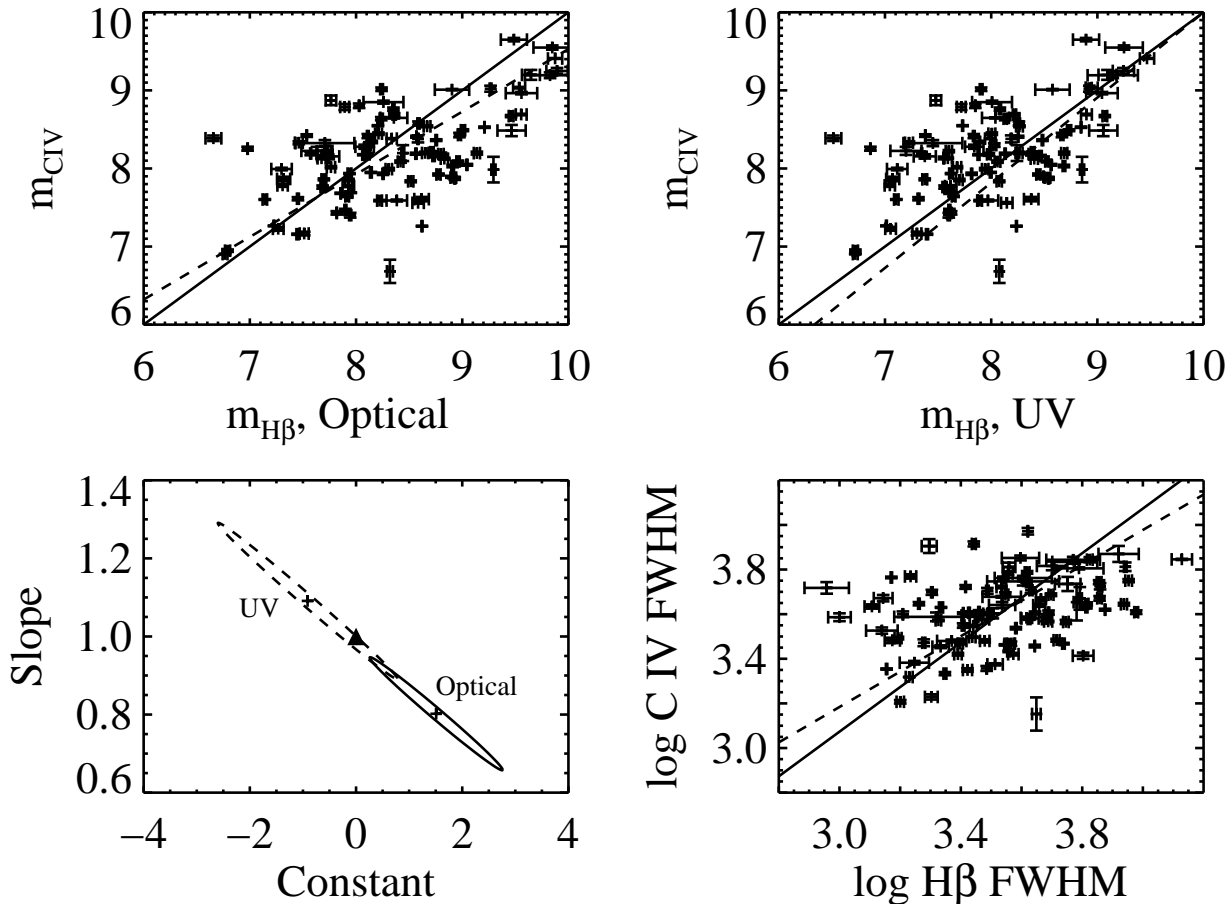


Fig. 6.— Plots comparing the $H\beta$ -based mass estimates with the C IV-based ones. The values of $\hat{m}_{H\beta}$ for the top left plot are calculated from the optical $R-L$ relationship, while the values of $\hat{m}_{H\beta}$ for the top right plot assume $R_{H\beta} \propto L_{1450}^{1/2}$. The error bars denote the propagated measurement errors in \hat{m} resulting from the measurement errors in the line widths and continuum luminosities. The solid lines are a 1:1 relationship and the dashed lines are the BCES bisector fits. The bottom left plot shows the 99% (2.6σ) confidence regions for the BCES bisector fits comparing \hat{m}_{CIV} with $\hat{m}_{H\beta}$. The solid contour correspond to $\hat{m}_{H\beta}$ calculated from the optical $R_{H\beta}-L$ relationship, and the dashed contour when $\hat{m}_{H\beta}$ is calculated from the UV one. The crosses mark the best-fit values, and the triangle marks the values expected for a 1:1 relationship. The bottom right plot shows a comparison between the $H\beta$ and C IV $FWHM$. The solid line is the best fit $FWHM_{H\beta} \propto FWHM_{CIV}$ relationship, and the dashed line is the BCES bisector fit.

Table 1. Object List

Object	RA (J2000)	DEC (J2000)	Redshift	$\log(M_{BH}/M_{\odot})^a$	Rad. Type ^b	Instrument
MRK 335	00 06 19.5	+20 12 10.5	0.025	6.41 ± 0.11	Quiet	FOS
PG 0026+129	00 29 13.7	+13 16 03.8	0.142	7.85 ± 0.10	Quiet	FOS
PG 0052+251	00 54 52.1	+25 25 39.3	0.155	7.82 ± 0.08	Quiet	FOS
FAIRALL9	01 23 45.7	-58 48 21.8	0.046	7.66 ± 0.09	Quiet	FOS
MRK 590	02 14 33.6	-00 46 00.1	0.027	6.93 ± 0.06	Quiet	IUE
3C 120	04 33 11.1	+05 21 15.6	0.033	7.00 ± 0.21^c	Loud	IUE
ARK 120	05 16 11.4	-00 08 59.4	0.033	7.43 ± 0.05	Quiet	FOS
MRK 79	07 42 32.8	+49 48 34.7	0.0221	6.97 ± 0.11	Quiet	IUE
PG 0804+761	08 10 58.6	+76 02 42.0	0.1000	8.10 ± 0.05	Quiet	IUE
MRK 110	09 25 12.9	+52 17 10.5	0.0352	6.65 ± 0.10	Quiet	IUE
PG 0953+414	09 56 52.4	+41 15 23.0	0.2341	7.69 ± 0.09	Quiet	FOS
NGC 3516	11 06 47.5	+72 34 06.9	0.0088	6.88 ± 0.14	Quiet	FOS
NGC 3783	11 39 01.7	-37 44 18.9	0.009	6.73 ± 0.07	Quiet	FOS
3C 273.0	12 29 06.7	+02 03 09.0	0.1583	8.20 ± 0.09	Loud	FOS
PG 1307+085	13 09 47.0	+08 19 49.8	0.1550	7.90 ± 0.12	Quiet	FOS
MRK 279	13 53 03.4	+69 18 29.6	0.0304	6.80 ± 0.26	Quiet	STIS
NGC 5548	14 17 59.5	+25 08 12.4	0.0171	7.08 ± 0.01	Quiet	FOS
PG 1426+015	14 29 06.6	+01 17 06.5	0.0864	8.37 ± 0.12	Quiet	IUE
MRK 817	14 36 22.1	+58 47 39.4	0.0314	6.95 ± 0.06	Quiet	IUE
PG 1613+658	16 13 57.2	+65 43 09.6	0.1290	7.70 ± 0.20^c	Quiet	IUE
PG 1617+175	16 20 11.3	+17 24 27.7	0.1124	8.03 ± 0.10	Quiet	IUE
3C 390.3	18 42 08.8	+79 46 17.0	0.0560	7.71 ± 0.09	Loud	FOS
MRK 509	20 44 09.8	-10 43 24.5	0.0350	7.41 ± 0.03	Quiet	FOS
PG 2130+099	21 32 27.8	+10 08 19.5	0.0629	7.91 ± 0.05	Quiet	GHRS
NGC 7469	23 03 15.6	+08 52 26.4	0.0163	6.34 ± 0.04	Quiet	FOS

^aBlack hole masses are from Peterson et al. (2004), assuming $f = 1$.

^bThe radio type is either radio loud or radio quiet.

^cThe standard errors in M_{BH} for 3C 120 and PG 1613+658 were estimated by averaging the upper and lower uncertainties listed by Peterson et al. (2004).

Table 2. Log of New Observations

Object	RA (J2000)	DEC (J2000)	Redshift	Date	Instrument	Exp. Time (s)
Q 0003+0146	00 05 47.6	+02 03 02.2	0.234	Oct 06, 2002	Bok B&C	1800
Q 0017+0209	00 20 25.1	+02 26 25.3	0.401	Oct 06, 2002	Bok B&C	2700
PKS 0044+030	00 47 05.9	+03 19 54.9	0.624	Oct 06, 2002	Bok B&C	1800
Q 0100+0205	01 03 13.0	+02 21 10.4	0.394	Oct 06, 2002	Bok B&C	2700
Q 0115+027	01 18 18.5	+02 58 05.9	0.672	Oct 06, 2002	Bok B&C	3600
3C 57	02 01 57.2	-11 32 33.7	0.669	Oct 06, 2002	Bok B&C	1800
PKS 0214+10	02 17 07.7	+11 04 09.6	0.408	Oct 06, 2002	Bok B&C	2700
IR 0450-2958	04 52 30.0	-29 53 35.0	0.286	Oct 06, 2002	Bok B&C	207
3C 232	09 58 21.0	+32 24 02.2	0.533	May 15, 2002	Bok B&C	1800
4C 41.21	10 10 27.5	+41 32 39.1	0.611	May 15, 2002	Bok B&C	1800
B2 1028+313	10 30 59.1	+31 02 56.0	0.178	May 15, 2002	Bok B&C	1800
MC 1104+167	11 07 15.0	+16 28 02.4	0.632	May 15, 2002	Bok B&C	1800
Q 1132-0302	11 35 04.9	-03 18 52.5	0.237	May 14, 2002	Bok B&C	1800
Q 1150+497	11 53 24.5	+49 31 08.6	0.334	May 14, 2002	Bok B&C	1200
TEX 1156+213	11 59 26.2	+21 06 56.2	0.349	May 15, 2002	Bok B&C	2100
MRK 205	12 21 44.0	+75 18 38.1	0.070	May 15, 2002	Bok B&C	1800
Q 1230+0947	12 33 25.8	+09 31 23.0	0.420	Mar 20, 2004	Bok B&C	1800
Q 1317-0142	13 19 50.3	-01 58 04.6	0.225	May 14, 2002	Bok B&C	900
PG 1333+176	13 36 02.0	+17 25 13.0	0.554	May 15, 2002	Bok B&C	2100
Q 1340-0038	13 42 51.6	-00 53 46.0	0.326	May 14, 2002	Bok B&C	1200
Q 1401+0951	14 04 10.6	+09 37 45.5	0.441	May 15, 2002	Bok B&C	1800
Q 1425+2003	14 27 25.0	+19 49 52.3	0.111	May 14, 2002	Bok B&C	900
PKS 1451-375	14 54 27.4	-37 47 34.2	0.314	Jul 17, 2004	IMACS	2700
PG 1538+477	15 39 34.8	+47 35 31.6	0.770	May 14, 2002	Bok B&C	1500
PKS 2128-12	21 31 35.4	-12 07 05.5	0.501	Oct. 06, 2002	Bok B&C	1800
PKS 2135-147	21 37 45.2	-14 32 55.8	0.200	May 15, 2002	Bok B&C	900
Q 2141+175	21 43 35.6	+17 43 49.1	0.213	May 15, 2002	Bok B&C	1200
PKS 2243-123	22 46 18.2	-12 06 51.2	0.630	Oct 06, 2002	Bok B&C	1800
PKS 2352-342	23 55 25.6	-33 57 55.8	0.706	Jul 17, 2004	IMACS	1800

Table 3. Continuum and Fe Emission Fitting Windows

	1	2	3	4	5	6
UV	$\lambda\lambda 1350\text{--}1365$	$\lambda\lambda 1427\text{--}1500$	$\lambda\lambda 1760\text{--}1860$	$\lambda\lambda 1950\text{--}2300$	$\lambda\lambda 2470\text{--}2755$	$\lambda\lambda 2855\text{--}3010$
Optical	$\lambda\lambda 3535\text{--}3700$	$\lambda\lambda 4100\text{--}4200$	$\lambda\lambda 4400\text{--}4700$	$\lambda\lambda 5100\text{--}6200$	$\lambda\lambda 6800\text{--}7534$...

Table 4. Continuum and C IV Emission Line Parameters

Object	$\log \lambda L_\lambda(1549 \text{ \AA})$ ergs cm ⁻² sec ⁻¹	<i>FWHM</i> 1000 km s ⁻¹	σ_* 1000 km s ⁻¹	<i>EW</i> Å	Δv 1000 km s ⁻¹	μ 1000 km s ⁻¹	α
MRK 335	44.38	2.094	1.856	71.82	0.368	0.141	-0.45
PG0026+12	45.19	1.971	5.263	52.45	0.054	-0.99	-0.85
0052+2509	45.39	5.762	4.544	120.4	-0.63	-0.51	-0.29
FAIRALL9	44.39	2.686	2.633	193.0	-0.19	-0.02	-0.72
MRK 590	43.35	2.846	1.818	185.2	-0.72	-1.21	-0.80
3C 120	44.56	5.040	2.813	148.3	-1.34	-0.87	-0.77
ARK 120	43.91	4.127	3.124	70.0	-0.00	0.647	-0.95
MRK 79	43.68	4.615	2.891	112.4	-0.41	-0.68	-0.73
PG 0804+761	45.26	3.608	3.307	62.63	-0.41	-1.20	-0.79
MRK 110	43.77	3.468	2.117	185.0	0.819	0.437	-0.79
PG0953+414	45.49	3.114	4.339	95.38	-1.20	0.210	-0.25
NGC 3516	42.31	3.512	2.480	327.9	0.054	-0.47	-2.05
NGC 3783	43.23	2.376	2.527	110.8	0.054	-0.21	-0.51
3C 273.0	46.28	3.659	3.285	31.24	-1.70	-0.64	-0.57
1307+0835	45.08	4.054	3.395	96.97	0.431	0.339	-0.35
MRK 279	44.32	3.057	3.201	110.2	-0.85	-1.00	-0.29
NGC 5548	43.49	3.490	3.278	202.2	0.431	0.214	-0.69
PG 1426+015	45.21	5.398	4.422	43.81	-0.10	-0.00	-0.61
MRK 817	44.13	4.192	3.719	66.52	-0.10	0.153	-0.94
PG 1613+658	45.14	5.869	5.099	81.43	-0.10	1.562	-0.79
PG 1617+175	44.69	7.842	2.906	50.60	0.201	0.947	-0.75
3C390.3	43.81	6.325	5.113	138.2	-0.13	-0.78	1.62
MRK509	44.68	4.313	3.722	128.3	-0.95	-0.13	-0.77
PG 2130+099	44.60	2.200	1.785	58.36	-0.78	-0.94	-0.78
NGC 7469	43.29	2.822	2.420	161.3	-0.07	0.028	-1.75

Table 5. Black Hole Mass Estimates

RA (J2000)	DEC (J2000)	z	$\log M_{BH}^{H\beta}/M_{\odot}^a$	$\log M_{BH}^{CIV}/M_{\odot}$	$\log M_{BH}^{BL}/M_{\odot}^b$
00 05 47.6	+02 03 02.2	0.234	7.32 ± 0.43	7.61 ± 0.40	7.47 ± 0.29
00 05 59.2	+16 09 49.1	0.450	8.38 ± 0.43	8.18 ± 0.40	8.27 ± 0.29
00 06 19.5	+20 12 10.3	0.025	6.72 ± 0.43	6.90 ± 0.40	6.82 ± 0.29
00 20 25.1	+02 26 25.3	0.401	7.23 ± 0.43	8.33 ± 0.40	7.82 ± 0.29
00 29 13.7	+13 16 03.8	0.142	7.30 ± 0.43	7.17 ± 0.40	7.23 ± 0.29
00 47 05.9	+03 19 54.9	0.624	9.07 ± 0.43	8.67 ± 0.40	8.86 ± 0.29
00 52 02.4	+01 01 29.3	2.270	9.47 ± 0.44	9.41 ± 0.40	9.44 ± 0.29
00 52 33.7	+01 40 40.6	2.307	9.25 ± 0.46	9.55 ± 0.40	9.42 ± 0.30
00 54 52.1	+25 25 39.3	0.155	7.89 ± 0.43	8.34 ± 0.40	8.13 ± 0.29
01 03 13.0	+02 21 10.4	0.394	8.47 ± 0.43	8.16 ± 0.40	8.30 ± 0.29
01 18 18.5	+02 58 05.9	0.672	8.38 ± 0.44	7.61 ± 0.40	7.96 ± 0.29
01 23 45.7	-58 48 21.8	0.047	7.40 ± 0.43	7.16 ± 0.40	7.27 ± 0.29
01 26 42.8	+25 59 01.3	2.370	9.24 ± 0.44	9.25 ± 0.40	9.25 ± 0.30
01 57 35.0	+74 42 43.2	2.338	9.10 ± 0.44	9.20 ± 0.41	9.15 ± 0.30
02 01 57.2	-11 32 33.7	0.669	8.01 ± 0.47	8.85 ± 0.40	8.49 ± 0.30
02 17 07.7	+11 04 09.6	0.408	8.69 ± 0.43	8.20 ± 0.40	8.42 ± 0.29
02 59 05.6	+00 11 21.9	3.366	8.95 ± 0.43	9.03 ± 0.40	8.99 ± 0.29
03 04 49.9	-00 08 13.4	3.294	8.90 ± 0.43	8.69 ± 0.40	8.79 ± 0.29
03 51 28.6	-14 29 09.1	0.616	8.92 ± 0.43	9.02 ± 0.40	8.98 ± 0.29
04 05 34.0	-13 08 14.1	0.571	8.56 ± 0.43	8.05 ± 0.40	8.29 ± 0.29
04 07 48.4	-12 11 36.0	0.574	8.25 ± 0.43	8.41 ± 0.40	8.34 ± 0.29
04 17 16.8	-05 53 45.9	0.781	9.04 ± 0.45	8.96 ± 0.40	9.00 ± 0.30
04 41 17.3	-43 13 43.7	0.593	8.08 ± 0.43	7.84 ± 0.40	7.95 ± 0.29
04 52 30.0	-29 53 35.0	0.286	7.37 ± 0.43	7.86 ± 0.40	7.64 ± 0.29
04 56 08.9	-21 59 09.4	0.534	8.73 ± 0.43	8.49 ± 0.40	8.60 ± 0.29
07 45 41.7	+31 42 55.7	0.462	8.27 ± 0.43	8.54 ± 0.40	8.41 ± 0.29
08 40 47.6	+13 12 23.7	0.684	8.06 ± 0.43	8.09 ± 0.40	8.07 ± 0.29
08 53 34.2	+43 49 01.0	0.513	7.84 ± 0.43	8.41 ± 0.40	8.15 ± 0.29
09 19 57.7	+51 06 10.0	0.553	8.26 ± 0.43	8.58 ± 0.40	8.43 ± 0.29
09 50 48.4	+39 26 51.0	0.206	8.53 ± 0.43	7.88 ± 0.40	8.18 ± 0.29
09 56 52.4	+41 15 23.0	0.239	7.70 ± 0.43	7.85 ± 0.40	7.78 ± 0.29
09 58 21.0	+32 24 02.2	0.533	7.48 ± 0.43	8.87 ± 0.40	8.22 ± 0.30
10 04 02.6	+28 55 35.0	0.329	6.86 ± 0.43	8.25 ± 0.40	7.61 ± 0.29
10 04 20.1	+05 13 00.0	0.161	7.60 ± 0.43	7.40 ± 0.40	7.49 ± 0.29
10 10 27.5	+41 32 39.1	0.611	7.99 ± 0.43	8.38 ± 0.40	8.20 ± 0.29
10 30 59.1	+31 02 56.0	0.178	7.97 ± 0.44	7.59 ± 0.40	7.76 ± 0.30
10 51 51.5	+00 51 18.1	0.357	7.88 ± 0.43	8.18 ± 0.40	8.04 ± 0.29
11 04 13.9	+76 58 58.2	0.311	8.44 ± 0.43	7.92 ± 0.40	8.16 ± 0.29
11 06 31.8	+00 52 53.4	0.425	8.67 ± 0.43	8.43 ± 0.40	8.54 ± 0.29
11 06 33.5	-18 21 24.0	2.319	8.89 ± 0.45	9.65 ± 0.40	9.31 ± 0.30
11 07 15.0	+16 28 02.4	0.632	8.04 ± 0.45	8.65 ± 0.40	8.38 ± 0.30
11 18 30.3	+40 25 55.0	0.154	7.82 ± 0.43	7.93 ± 0.40	7.88 ± 0.29
11 19 08.7	+21 19 18.0	0.176	7.55 ± 0.43	8.13 ± 0.40	7.87 ± 0.29
11 24 39.2	+42 01 45.2	0.234	7.61 ± 0.43	7.47 ± 0.40	7.53 ± 0.29
11 35 04.9	-03 18 52.5	0.237	7.07 ± 0.43	7.87 ± 0.40	7.50 ± 0.29
11 39 57.1	+65 47 49.4	0.652	7.60 ± 0.43	8.22 ± 0.40	7.93 ± 0.29
11 41 21.7	+01 48 03.3	0.383	7.20 ± 0.45	8.23 ± 0.40	7.77 ± 0.30
11 47 18.0	-01 32 07.7	0.382	8.08 ± 0.43	6.68 ± 0.43	7.37 ± 0.30
11 53 24.5	+49 31 08.6	0.334	7.68 ± 0.43	8.02 ± 0.40	7.86 ± 0.29
11 58 39.9	+62 54 28.1	0.594	7.45 ± 0.51	8.32 ± 0.40	7.99 ± 0.32
11 59 26.2	+21 06 56.2	0.349	8.69 ± 0.43	8.03 ± 0.40	8.33 ± 0.29
12 04 42.2	+27 54 12.0	0.165	8.24 ± 0.43	7.26 ± 0.40	7.71 ± 0.29
12 14 17.7	+14 03 12.3	0.080	6.72 ± 0.43	6.95 ± 0.40	6.84 ± 0.29
12 19 20.9	+06 38 38.4	0.334	8.00 ± 0.43	7.95 ± 0.40	7.97 ± 0.29

Table 5—Continued

RA (J2000)	DEC (J2000)	z	$\log M_{BH}^{H\beta}/M_{\odot}^a$	$\log M_{BH}^{CIV}/M_{\odot}$	$\log M_{BH}^{BL}/M_{\odot}^b$
12 21 44.0	+75 18 38.1	0.070	7.89 ± 0.43	7.59 ± 0.40	7.73 ± 0.29
12 31 20.6	+07 25 52.8	2.391	9.14 ± 0.49	9.19 ± 0.40	9.17 ± 0.31
12 33 25.8	+09 31 23.0	0.420	7.98 ± 0.43	8.18 ± 0.40	8.09 ± 0.29
13 01 12.9	+59 02 06.9	0.472	7.91 ± 0.43	9.01 ± 0.40	8.50 ± 0.29
13 05 33.0	-10 33 20.4	0.286	8.19 ± 0.43	8.38 ± 0.40	8.29 ± 0.29
13 09 47.0	+08 19 49.8	0.155	8.54 ± 0.43	7.87 ± 0.40	8.18 ± 0.29
13 12 17.7	+35 15 21.0	0.184	7.62 ± 0.43	7.43 ± 0.40	7.52 ± 0.29
13 19 50.3	-01 58 04.6	0.225	7.05 ± 0.43	7.23 ± 0.40	7.15 ± 0.29
13 23 49.5	+65 41 48.0	0.168	7.11 ± 0.43	7.60 ± 0.40	7.37 ± 0.29
13 36 02.0	+17 25 13.0	0.554	7.72 ± 0.43	8.79 ± 0.40	8.29 ± 0.29
13 42 51.6	-00 53 46.0	0.326	8.27 ± 0.43	8.20 ± 0.40	8.23 ± 0.29
13 57 04.5	+19 19 06.6	0.719	7.12 ± 0.44	7.99 ± 0.40	7.60 ± 0.30
14 04 10.6	+09 37 45.5	0.441	9.06 ± 0.45	8.49 ± 0.41	8.74 ± 0.30
14 05 16.2	+25 55 33.6	0.164	7.35 ± 0.43	8.19 ± 0.40	7.80 ± 0.29
14 17 00.9	+44 56 06.0	0.114	7.61 ± 0.43	7.68 ± 0.40	7.65 ± 0.29
14 19 03.9	-13 10 45.0	0.129	7.56 ± 0.43	7.76 ± 0.40	7.67 ± 0.29
14 27 25.0	+19 49 52.3	0.111	8.03 ± 0.43	8.30 ± 0.40	8.17 ± 0.29
14 27 35.7	+26 32 15.0	0.366	7.85 ± 0.43	8.80 ± 0.40	8.36 ± 0.29
14 29 43.1	+47 47 26.0	0.221	7.65 ± 0.43	7.64 ± 0.40	7.64 ± 0.29
14 42 07.5	+35 26 22.9	0.077	7.01 ± 0.43	7.26 ± 0.40	7.15 ± 0.29
14 46 45.9	+40 35 07.1	0.267	7.38 ± 0.43	8.42 ± 0.40	7.94 ± 0.29
14 54 27.4	-37 47 34.2	0.314	7.62 ± 0.43	7.93 ± 0.40	7.79 ± 0.29
15 14 43.5	+36 50 51.0	0.371	7.84 ± 0.44	8.28 ± 0.40	8.08 ± 0.30
15 39 34.8	+47 35 31.6	0.770	8.58 ± 0.46	9.01 ± 0.40	8.82 ± 0.30
15 45 30.3	+48 46 07.9	0.400	7.73 ± 0.43	8.55 ± 0.40	8.17 ± 0.29
15 47 43.5	+20 52 16.4	0.264	8.39 ± 0.43	8.21 ± 0.40	8.29 ± 0.29
16 14 13.2	+26 04 16.2	0.131	7.05 ± 0.43	7.78 ± 0.40	7.44 ± 0.29
16 20 21.8	+17 36 24.0	0.555	8.22 ± 0.43	8.69 ± 0.40	8.47 ± 0.29
16 27 56.1	+55 22 31.0	0.133	8.49 ± 0.43	7.89 ± 0.40	8.17 ± 0.29
16 42 58.8	+39 48 36.9	0.595	8.01 ± 0.43	8.45 ± 0.40	8.24 ± 0.29
17 04 41.3	+60 44 30.0	0.371	7.37 ± 0.44	8.15 ± 0.40	7.80 ± 0.30
18 21 59.4	+64 21 07.5	0.297	8.85 ± 0.43	8.53 ± 0.40	8.68 ± 0.29
19 27 48.5	+73 58 02.0	0.302	8.13 ± 0.43	8.19 ± 0.40	8.16 ± 0.29
20 44 09.8	-10 43 24.5	0.035	7.64 ± 0.43	7.69 ± 0.40	7.66 ± 0.29
21 31 35.4	-12 07 05.5	0.501	8.13 ± 0.43	8.64 ± 0.40	8.40 ± 0.29
21 37 45.2	-14 32 55.8	0.200	8.86 ± 0.43	7.99 ± 0.43	8.42 ± 0.31
21 43 35.6	+17 43 49.1	0.213	8.24 ± 0.43	8.20 ± 0.41	8.22 ± 0.30
22 03 15.0	+31 45 37.7	0.297	8.08 ± 0.43	8.76 ± 0.40	8.45 ± 0.29
22 46 18.2	-12 06 51.2	0.630	8.41 ± 0.43	8.13 ± 0.40	8.26 ± 0.29
22 54 05.8	-17 34 55.0	0.068	8.15 ± 0.43	7.56 ± 0.40	7.83 ± 0.29
22 54 10.4	+11 36 38.9	0.323	7.59 ± 0.43	8.13 ± 0.40	7.88 ± 0.29
23 03 43.5	-68 07 37.1	0.512	7.62 ± 0.43	7.77 ± 0.40	7.70 ± 0.29
23 11 17.8	+10 08 16.2	0.432	8.48 ± 0.43	8.36 ± 0.40	8.42 ± 0.29
23 46 36.9	+09 30 46.0	0.672	7.94 ± 0.43	7.99 ± 0.40	7.97 ± 0.29
23 51 56.0	-01 09 13.7	0.174	8.52 ± 0.43	8.09 ± 0.40	8.29 ± 0.29
23 55 25.6	-33 57 55.8	0.706	6.51 ± 0.44	8.39 ± 0.40	7.53 ± 0.30

Note. — The 1σ uncertainties include the contributions from measurement error in the line widths and continuum luminosities, and from the intrinsic uncertainty in \hat{m} .

^aThe $H\beta$ -based mass estimates are for the UV $R_{H\beta}$ - L relationship. The 1σ errors were calculated assuming $\sigma_{H\beta} = 0.43$ dex (Vestergaard & Peterson 2006).

^b M_{BH}^{BL} is a weighted average of the $H\beta$ - and C IV-based mass estimates.